

A rigid axle based molecular rotaxane channel facilitates K^+/Cl^- cotransport across a lipid membrane

Shihao Pang, Xiaonan Sun, Zexin Yan, Chuantao Wang, Kai Ye, Shinan Ma, Linyong Zhu, Chunyan Bao *

Key Laboratory for Advanced Materials and Joint International Research Laboratory of Precision Chemistry and Molecular Engineering, Feringa Nobel Prize Scientist Joint Research Center, Frontiers Science Center for Materiobiology and Dynamic Chemistry, Institute of Fine Chemicals, School of Chemistry and Molecular Engineering, East China University of Science and Technology, Shanghai 200237, China

1. General materials and characterizations.

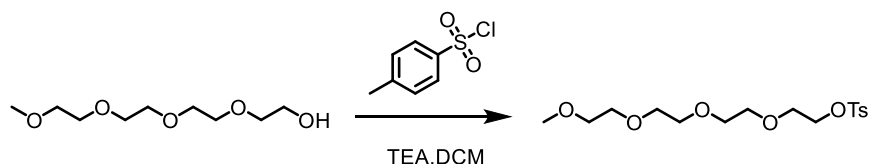
All raw materials were obtained from commercial suppliers and all solvents were used without further purification unless otherwise. All air- or moisture-sensitive reactions were performed using oven-dried solvent under an inert atmosphere of dry argon. Egg yolk phosphatidylcholine (EYPC) and 1,2-diphytanoyl-sn-glycero-3-phosphocholine (DPhPC) were obtained from Avanti Polar lipids as powder. 8-hydroxy-1, 3, 6-pyrenetrisulfonate (HPTS), N, N'-dimethyl-9,9'-biacridinium dinitrate (lucigenin) and Triton X-100 were obtained from Sigma Aldrich and used without further purification.^{1,2}

Proton and carbon nuclear magnetic resonance spectra (1H , ^{13}C NMR) were recorded on a Bruker Avance 400 MHz / 600 MHz spectrometer were recorded on a Bruker AV-600 spectrometer. Chemical shifts were reported in parts per million (ppm) downfield from the Me_4Si resonance which was used as the internal standard when recording 1H NMR spectra. Mass spectra were recorded on a Micro-mass GCTTM and a Micro-mass LCTTM. Fluorescence measurements were performed on a Varian Cary Eclipses fluorescence spectrometer equipped with a stirrer and a temperature controller (kept at 25 °C unless otherwise noted). A mini-Extruder used for the preparation of large unilamellar vesicles (LUVs) was purchased from Avanti Polar lipids. The size of EYPC vesicles was determined using a DelasTM Nano Submicron Particle Size and Zeta Potential Particle Analyzer (Bechman Coulter Inc., USA). Preparative reverse phase HPLC was performed using a waters 2454 Multisolvant Delivery System with a Waters

2489 UV/visible detector operating at 254 nm.

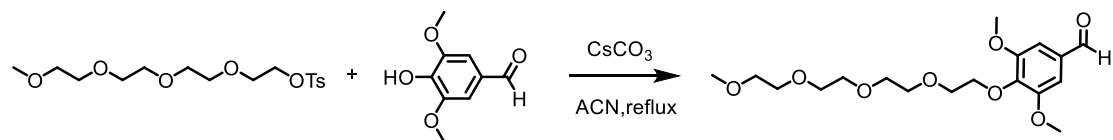
2. Synthesis of Compounds

2.1 Synthesis of A4



Scheme S1. Synthesis of compound **A1**.

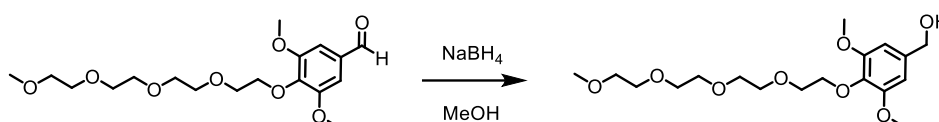
Compound A1: To a solution of tetraethyleneglycol monomethyl ether (10.0 g, 48.0 mmol) in dry CH_2Cl_2 (100 mL) was added p-tosyl chloride (10.1 g, 52.8 mmol) and triethylamine (16.7 mL, 120 mmol) in sequence. The mixture was stirred at room temperature for 8 h. TLC showed complete consumption of the starting material, and the reaction was extracted with DCM (50 mL \times 3) and the combined organic layers were dried over Na_2SO_4 and concentrated. The product was purified by column chromatography (SiO_2 , CH_2Cl_2) to afford faint yellow oil compound **A1** (16.54 g, 95% yield). ^1H NMR (400 MHz, CDCl_3 - d_1) δ 7.74 – 7.68 (m, 2H), 7.27 (d, J = 8.1 Hz, 2H), 4.07 (dd, J = 5.7, 3.9 Hz, 2H), 3.69 – 3.40 (m, 17H), 3.29 (s, 3H), 2.37 (s, 3H). ^{13}C NMR (101 MHz, CDCl_3 - d_1) δ 144.80, 133.17, 132.87, 129.82, 127.88, 77.62, 77.31, 76.99, 71.83, 70.60, 70.49, 70.42, 70.41, 69.29, 68.55, 58.92, 21.57. MS (ESI): m/z : Calcd. For $\text{C}_{16}\text{H}_{26}\text{O}_7\text{S}$ $[\text{M}+\text{H}]^+$: 363.4370; found: 363.4392.



Scheme S2. Synthesis of compound **A2**

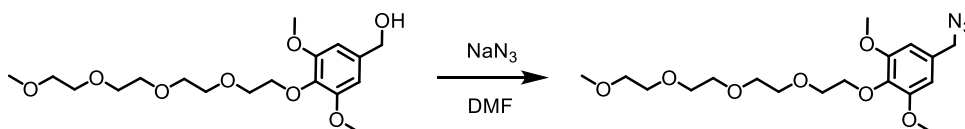
Compound A2: To a solution of 3,5-dimethoxy-4-hydroxybenzaldehyde (2.5 g, 13.5 mmol) in dry MeCN (100 mL) was added **A1** (6.0 g, 17.0 mmol) and CsCO_3 (13.4 g, 41.0 mmol). The mixture was refluxed at 90 °C for 6h. Then the mixture was cooled to room temperature and CsCO_3 was filtered. The solvent was removed under vacuum.

The crude product was further purified by column chromatography (SiO₂, CH₂Cl₂/MeOH=150:1) to yield product A2 as yellow oil (4.0 g, 82% yield). ¹H NMR (400 MHz, DMSO-*d*₆) δ 9.88 (s, 1H), 7.25 (s, 2H), 4.12 – 4.05 (m, 2H), 3.86 (s, 6H), 3.70 – 3.63 (m, 2H), 3.61 – 3.46 (m, 10H), 3.45 – 3.38 (m, 2H), 3.23 (s, 3H). ¹³C NMR (101 MHz, CDCl₃-*d*₁) δ 191.20, 191.06, 153.68, 153.56, 142.54, 131.70, 131.68, 129.01, 106.70, 106.41, 72.28, 71.80, 70.66, 70.60, 70.55, 70.51, 70.46, 70.40, 70.37, 70.32. MS (ESI): m/z: Calcd. For C₁₈H₂₈O₈ [M+Na]⁺: 395.4140; found: 395.4182.



Scheme S3. Synthesis of compound **A3**

Compound A3: To a solution of A2 (4.0 g, 11.0 mmol) in MeOH (100 mL) was added NaBH₄ (0.8 g, 21.1 mmol) under ice bath. After stirred at room temperature for 5 h, the reaction mixture was diluted with brine (30 mL×3) followed by extraction with DCM (30 mL×3). The combined organic layers were dried over anhydrous Na₂SO₄, filtered and concentrated to give the crude product. After purification by column chromatography (SiO₂, CH₂Cl₂/MeOH=150:1), compound A3 was obtained with 90% yield. ¹H NMR (400 MHz, CDCl₃-*d*₁) δ 6.51 (s, 2H), 5.25 (s, 1H), 4.53 (s, 2H), 4.05 (dd, J = 5.8, 4.5 Hz, 2H), 3.81 – 3.44 (m, 20H), 3.31 (s, 3H). ¹³C NMR (101 MHz, CDCl₃-*d*₁) δ 162.65, 153.35, 137.30, 137.01, 136.06, 103.72, 77.52, 77.41, 77.20, 76.89, 72.15, 71.89, 70.61, 70.57, 70.53, 70.45, 70.36, 65.14, 58.97, 56.02, 53.52, 36.53, 31.44. MS (ESI): m/z: Calcd. for C₁₈H₃₀O₈ [M+Na]⁺: 397.4300; found: 397.4310.

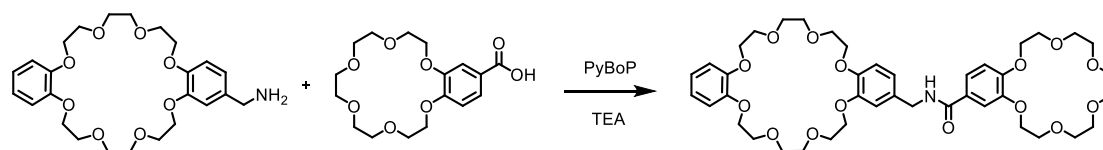


Scheme S4. Synthesis of compound **A4**.

Compound A4: To a solution of A3 (3.8 g, 10.0 mmol) in DMF (20 mL) was added NaN₃ (1.3 g, 20.0 mmol) carefully and refluxed at 70 °C for 12 h. Then the mixture was cooled to room temperature. The residue NaN₃ was filtered and quenched with H₂O. The solvent was removed under vacuum. The crude product was purified by column

chromatography (SiO₂, CH₂Cl₂/MeOH=200:1) to afford faint yellow oil compound A4 (2.6 g, 80% yield). ¹H NMR (400 MHz, CDCl₃-*d*₁) δ 6.49 (s, 2H), 4.26 (s, 2H), 4.11 (dd, *J* = 5.8, 4.5 Hz, 2H), 3.88 – 3.50 (m, 21H), 3.35 (s, 3H). ¹³C NMR (101 MHz, CDCl₃-*d*₁) δ 153.59, 136.95, 131.01, 105.18, 77.41, 77.09, 76.78, 72.21, 71.93, 70.64, 70.61, 70.58, 70.50, 70.38, 59.01, 58.35, 56.15, 55.13, 18.42. MS (ESI): *m/z*: Calcd. for C₁₈H₂₉N₃O₇ [M+Na]⁺: 422.4440; found: 422.1956.

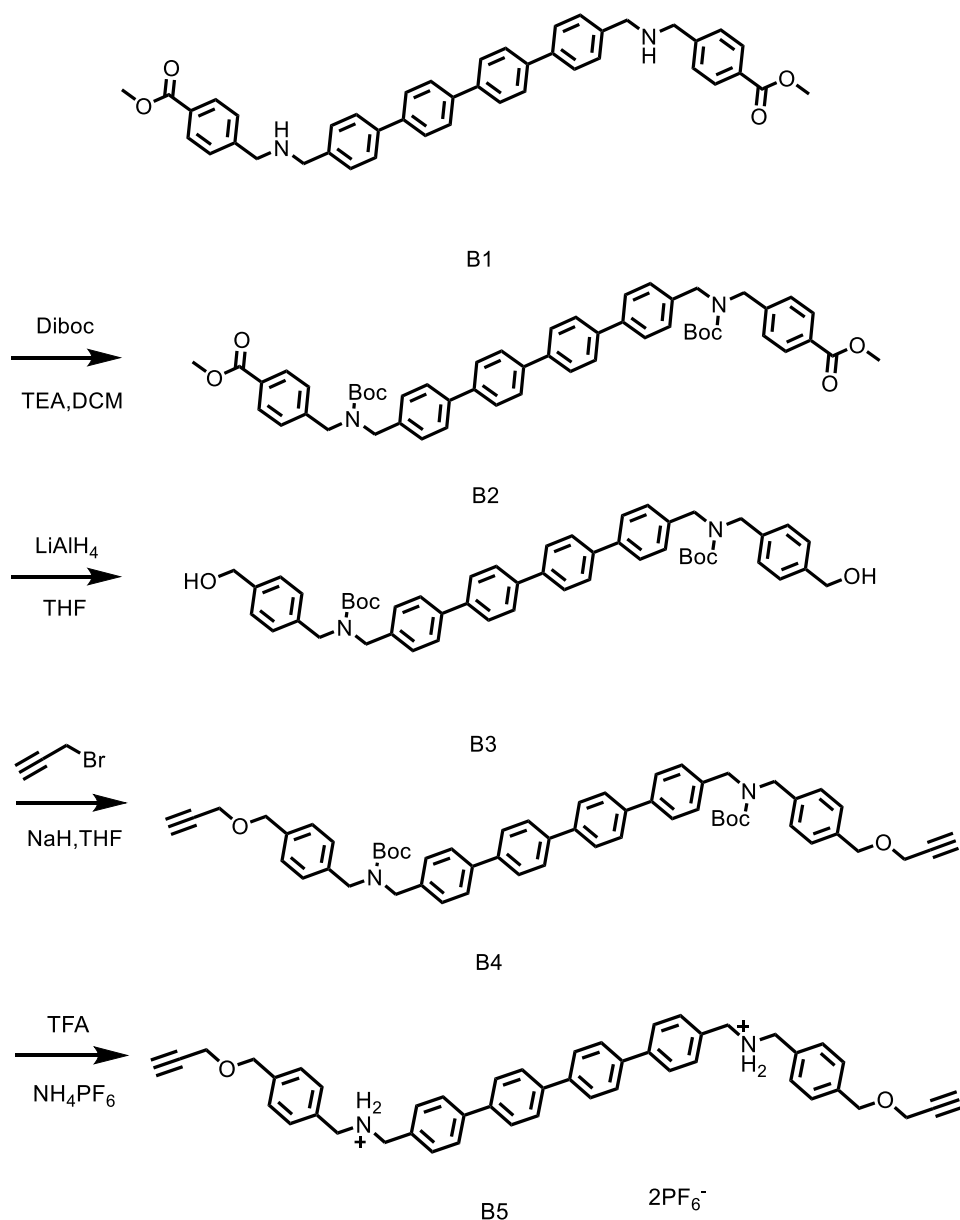
2.2 Synthesis compound NCE



Scheme S5. Synthesis of compound NCE.

Compound NCE: To a solution of 4-benzylamine - 24-crown-8 (2.0 g, 4.2 mmol) and 4-carboxyl-18-crown-6 (1.6 g, 4.5 mmol) in dry-DMF (10 mL) were added PyBoP (5.5 g, 8.4 mmol) and TEA (1.7 mL, 12.6 mmol) in sequence. The solution stirred at room temperature for 12 h. The solvent was removed under vacuum. The product was purified by column chromatography (SiO₂, CH₂Cl₂/MeOH=150:1) to afford white solid compound NCE (2.1 g, 60% yield). ¹H NMR (600 MHz, CD₃CN-*d*₃) δ 8.25 – 8.09 (m, 2H), 7.71 – 7.49 (m, 9H), 5.09 (d, *J* = 5.8 Hz, 2H), 4.91 – 4.68 (m, 12H), 4.51 – 3.92 (m, 56H), 3.75 (td, *J* = 6.6, 3.8 Hz, 10H), 3.21 (p, *J* = 1.9 Hz, 7H), 2.50 – 2.42 (m, 10H). ¹³C NMR (151 MHz, CD₃CN-*d*₃) δ 166.33, 148.82, 121.32, 120.36, 120.12, 114.72, 114.08, 113.95, 113.92, 113.76, 113.73, 113.66, 78.10, 77.88, 77.66, 70.69, 70.22, 70.15, 70.04, 69.98, 69.58, 69.54, 69.04, 68.90, 68.87, 68.77, 68.69, 42.89, 1.03, 0.89, 0.75, 0.61, 0.47, 0.46, 0.34, 0.20. MS (ESI): *m/z*: Calcd. for C₄₂H₅₇NO₁₅ [M+Na]⁺: 838.9100; found: 838.9110.

2.3 Synthesis compound B5



Scheme S6. Synthesis of compound **B5**.

Compound B1: Compound B1 was synthesized according to the literature procedure.³ ¹H NMR (400 MHz, CDCl₃-*d*₁) δ 7.95 (d, *J* = 8.0 Hz, 4H), 7.69 – 7.60 (m, 8H), 7.56 (d, *J* = 7.8 Hz, 4H), 7.38 (t, *J* = 7.4 Hz, 8H), 3.89 – 3.78 (m, 14H). ¹³C NMR (101 MHz, CDCl₃-*d*₁) δ 167.10, 145.72, 139.91, 139.53, 139.49, 139.29, 129.79, 128.89, 128.69, 128.05, 127.47, 127.40, 127.11, 77.37, 77.05, 76.73, 52.89, 52.83, 52.11. MS (ESI): *m/z*: Calcd. for C₄₄H₄₀N₂O₄ [M+Na]⁺: 683.8140; found: 683.8152.

Compound B2: To a solution of B1 (5.0 g, 7.6 mmol) in dry-CH₂Cl₂ (100 mL) was added di-*tert*-butyl dicarbonate (3.5 g, 15.9 mmol) and TEA (3.2 mL, 22.7 mmol) in

sequence. The mixture was stirred at room temperature for 6 h. The reaction was diluted with water (100 mL) and extracted with CH₂Cl₂ (30 mL×3). The combined organic layers were dried over anhydrous Na₂SO₄, filtered and concentrated to give the crude product, which was further purified by column chromatography (SiO₂, CH₂Cl₂) to obtain compound B2 (5.8 g, 95% yield). ¹H NMR (400 MHz, CDCl₃-*d*₁) δ 8.02 (d, *J* = 8.0 Hz, 4H), 7.72 (q, *J* = 8.2 Hz, 9H), 7.62 (d, *J* = 7.9 Hz, 4H), 7.35 – 7.27 (m, 9H), 4.52 (s, 4H), 4.42 (d, *J* = 10.7 Hz, 4H), 3.93 (s, 6H), 1.51 (d, *J* = 16.8 Hz, 19H). ¹³C NMR (101 MHz, CDCl₃-*d*₁) δ 166.95, 155.98, 139.80, 139.60, 136.91, 129.92, 129.17, 128.56, 128.00, 127.80, 127.49, 127.43, 127.24, 80.52, 77.38, 77.07, 76.75, 52.16, 28.46. MS (ESI): *m/z*: Calcd. for C₅₄H₅₆N₂O₈ [M+Na]⁺: 884.0480; found: 884.0420.

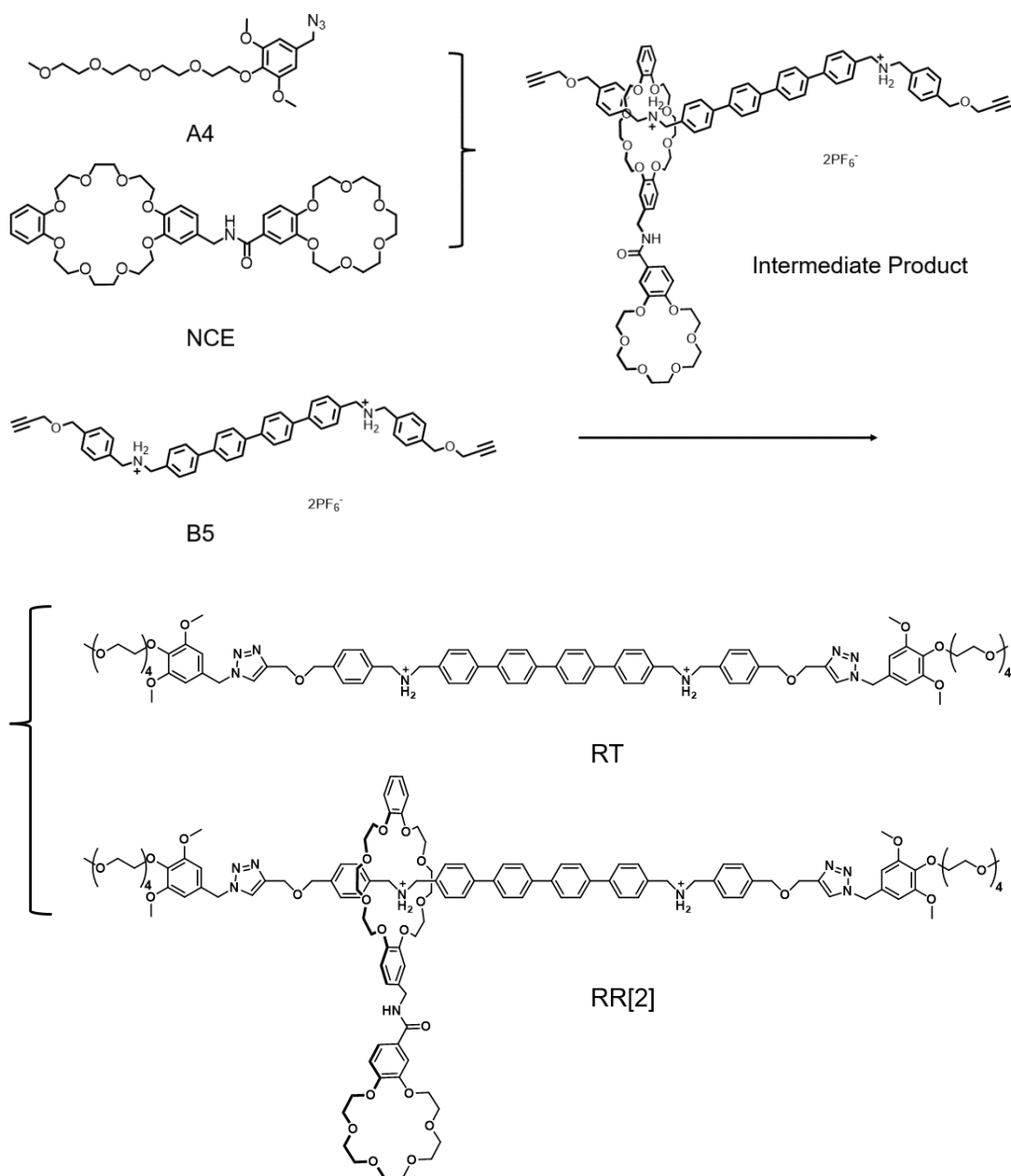
Compound B3: To a solution of B2 (5.0 g, 6.2 mmol) in dry-THF (100 mL) was added a suspension of 2.5M lithium aluminum hydride (7.0 mL, 17.4 mmol) dropwise under ice bath over 15 min. Then, the mixture was slowly warmed to room temperature and kept stirring for another 8 h. After the starting material was consumed completely (detected by TLC), the reaction was quenched with ice-water (10 mL) at 0 °C and then extracted with CHCl₃/iPrOH (3:1 v/v, 50 mL×3). The combined organic layers was dried over anhydrous Na₂SO₄ and then concentrated under reduced pressure. The obtained crude product was subsequently purified by column chromatography (SiO₂, CH₂Cl₂: MeOH= 150:1) to yield compound B3 (3.7 g, yield 80%). ¹H NMR (400 MHz, CDCl₃-*d*₁) δ 7.72 (q, *J* = 8.2 Hz, 9H), 7.62 (d, *J* = 7.9 Hz, 4H), 7.38 – 7.19 (m, 12H), 4.70 (s, 4H), 4.43 (d, *J* = 31.4 Hz, 8H), 1.52 (s, 18H). ¹³C NMR (101 MHz, CDCl₃-*d*₁) δ 156.08, 140.03, 139.79, 139.66, 139.56, 137.38, 137.22, 128.52, 128.28, 127.99, 127.68, 127.48, 127.42, 127.31, 127.19, 80.31, 77.39, 77.08, 76.76, 65.08, 49.09, 48.78, 28.51, 0.04. MS (ESI): *m/z*: Calcd. for C₅₂H₅₆N₂O₆ [M+Na]⁺: 828.0280; found: 828.0235.

Compound B4: To a solution of B3 (3.5 g, 4.3 mmol) in dry-THF (100 mL) was added NaH (1.0 g, 43.5 mmol) and 3-Bromo-1-propyne (2.6 g, 20.8 mmol) in sequence. The mixture was stirred at 0 °C for 30 min, and then was slowly warmed to room temperature. After 12 h reaction, the system was filtered, and the filter cake was quenched with absolute ethanol. The mixture was purified by column chromatography

(SiO₂, CH₂Cl₂) to yield compound B4 (3.1 g, yield 80%). ¹H NMR (400 MHz, CDCl₃-*d*₁) δ 8.02 – 7.61 (m, 12H), 7.43 – 7.15 (m, 8H), 4.51 (s, 4H), 4.38 (d, *J* = 16.0 Hz, 8H), 4.17 (d, *J* = 2.4 Hz, 4H), 1.42 (s, 18H). ¹³C NMR (101 MHz, CDCl₃-*d*₁) δ 156.06, 139.82, 139.66, 139.57, 137.81, 137.16, 136.34, 128.47, 128.22, 127.99, 127.59, 127.49, 127.42, 127.19, 80.26, 79.65, 77.40, 77.08, 76.76, 74.75, 71.33, 57.16, 49.20, 49.06, 48.78, 28.51, 0.05. MS (ESI): *m/z*: Calcd. for C₅₈H₆₀N₂O₆ [M+Na]⁺: 904.1260; found: 904.1240.

Compound B5: To a solution of B4 (2.0 g, 2.3 mmol) in dichloromethane (10 mL) was added TFA (2 mL). After the reaction mixture was stirred at room temperature for 4h, it was poured into saturated aqueous NH₄PF₆ (100 mL) and then extracted with dichloromethane (100 mL×3). The combined organics were washed with saturated aqueous NH₄PF₆ (100 mL), dried over anhydrous Na₂SO₄, and then concentrated under reduced pressure. The obtained crude product was reprecipitated with hexane to provide the desired white solid compound B5 (2.0 g, yield 90%). ¹H NMR (600 MHz, CD₃CN-*d*₃) δ 7.86 – 7.77 (m, 12H), 7.58 (d, *J* = 8.2 Hz, 4H), 7.51 – 7.42 (m, 8H), 4.60 (s, 4H), 4.29 (d, *J* = 10.8 Hz, 8H), 4.21 (d, *J* = 2.5 Hz, 4H), 2.77 (t, *J* = 2.4 Hz, 2H). ¹³C NMR (151 MHz, CD₃CN-*d*₃) δ 141.95, 140.21, 140.12, 139.51, 131.41, 130.90, 130.55, 130.40, 128.97, 128.09, 127.99, 127.90, 117.95, 80.24, 75.67, 71.27, 57.80, 51.73, 51.58, 1.52, 1.31, 1.10, 0.90, 0.69, 0.48, 0.28. MS (ESI): *m/z*: Calcd. for C₄₈H₄₆N₂O₂²⁺ [M+Na]⁺: 364.1774 ; found: 364.1740 .

2.4 Synthesis compounds RT and RR[2]



Scheme S7. Synthesis of compound **RT** & **RR[2]**.

Compound RT: To a solution of **B6** (50.0 mg, 0.051 mmol) in dry-DCM (1.5 mL) was added **A4** (43.1 mg, 0.108 mmol) and tetra kis(MeCN)copper(I) hexafluorophosphate (67.1 mg, 0.180 mmol). The obtained mixture was stirred at room temperature for 12 h. After removing the solvent under vacuum, the crude product was purified by column chromatography (SiO₂, CH₂Cl₂: MeOH=20:1) and a pale yellow powder compound **RT** was obtained (35 mg, yield 47%). ¹H NMR (600 MHz, CD₃CN-*d*₃) δ 7.79 – 7.71 (m, 10H), 7.67 – 7.63 (m, 4H), 7.45 (d, J = 7.9 Hz, 4H), 7.37 – 7.27 (m, 8H), 6.61 (s, 4H),

5.44 (s, 4H), 4.61 (s, 4H), 4.54 (s, 4H), 4.05 – 3.99 (m, 4H), 3.84 – 3.76 (m, 20H), 3.71 – 3.64 (m, 5H), 3.63 – 3.53 (m, 21H), 3.47 (dd, $J = 5.9, 3.5$ Hz, 4H), 3.28 (s, 6H). ^{13}C NMR (151 MHz, $\text{CD}_3\text{CN}-d_3$) δ 153.54, 144.96, 140.22, 139.73, 139.06, 138.66, 136.68, 131.16, 128.68, 128.09, 127.86, 127.25, 127.18, 126.64, 123.19, 105.50, 105.48, 78.11, 77.89, 77.67, 72.00, 71.75, 71.58, 70.19, 70.14, 70.09, 70.01, 63.20, 58.16, 58.14, 55.87, 53.74, 52.48, 52.33, 0.87, 0.73, 0.71, 0.59, 0.57, 0.46, 0.43, 0.29. MS (ESI): m/z : Calcd. for $\text{C}_{84}\text{H}_{104}\text{N}_8\text{O}_{16}^{2+}$ $[\text{M}-2\text{PF}_6]^{2+}$: 740.3780; found: 740.3820.

Compound RR[2]: To a solution of B6 (50.0 mg, 0.051 mmol) in dry-DCM (1.5 mL) was added NCE (62.9 mg, 0.077 mmol) and stirred at room temperature for 12 h to form pseudorotaxane. Then the mixture was added A4 (43.1 mg, 0.108 mmol) in DCM (1.0 mL). Tetrakis(MeCN)copper(I) hexafluorophosphate (67.1 mg, 0.180 mmol) in DCM (1.0 mL) was added into flask. The mixture was kept at room temperature for 12 h. The combined solvent was removed under vacuum. The crude product was purified by column chromatography (SiO_2 , CH_2Cl_2 : MeOH=20:1). The pale yellow powder compound **RR[2]** (24.8 mg, yield 21%). ^1H NMR (600 MHz, $\text{CD}_3\text{CN}-d_3$) δ 7.78 – 7.70 (m, 8H), 7.67 – 7.56 (m, 6H), 7.49 – 7.42 (m, 5H), 7.39 (dd, $J = 7.2, 3.0$ Hz, 4H), 7.33 (dd, $J = 12.4, 8.1$ Hz, 4H), 7.28 (d, $J = 8.1$ Hz, 2H), 7.12 (d, $J = 8.0$ Hz, 2H), 6.81 – 6.75 (m, 4H), 6.62 (d, $J = 2.4$ Hz, 4H), 5.43 (d, $J = 4.1$ Hz, 4H), 4.69 (ddd, $J = 13.5, 9.9, 4.5$ Hz, 4H), 4.59 (s, 2H), 4.52 (d, $J = 2.8$ Hz, 4H), 4.40 (s, 2H), 4.36 (dd, $J = 8.6, 6.1$ Hz, 2H), 4.12 (ddt, $J = 6.7, 4.5, 2.3$ Hz, 4H), 4.06 (ttt, $J = 9.2, 6.2, 5.7, 3.5$ Hz, 6H), 4.03 – 3.96 (m, 6H), 3.86 – 3.67 (m, 28H), 3.70 – 3.48 (m, 45H), 3.44 (ddd, $J = 6.2, 3.1, 1.5$ Hz, 4H), 3.23 (d, $J = 11.1$ Hz, 6H). ^{13}C NMR (151 MHz, $\text{CD}_3\text{CN}-d_3$) δ 153.54, 153.50, 147.41, 147.17, 144.93, 144.71, 136.82, 129.87, 129.28, 129.24, 128.76, 128.25, 128.14, 128.12, 127.89, 127.85, 127.61, 127.39, 127.31, 127.27, 127.19, 127.16, 126.69, 126.64, 123.47, 123.36, 123.26, 121.21, 120.29, 120.24, 117.16, 115.65, 115.60, 115.51, 114.23, 112.37, 112.30, 111.99, 111.93, 111.77, 105.57, 105.50, 105.43, 78.26, 78.12, 77.91, 77.69, 77.64, 71.99, 71.65, 71.52, 71.47, 70.68, 70.58, 70.56, 70.29, 70.24, 70.11, 70.08, 70.05, 70.03, 70.00, 69.93, 69.89, 69.87, 69.84, 69.64, 69.42, 69.35, 69.28, 69.02, 67.74, 63.15, 63.08, 58.04, 55.84, 53.71, 53.66, 52.40, 1.79, 1.58, 1.54, 1.52, 1.48, 1.45, 1.31, 1.31, 0.88, 0.74, 0.60, 0.46, 0.32, 0.31, 0.19, 0.05. MS (ESI): m/z :

Calcd. for $C_{126}H_{161}N_9O_{31}^{2+}$ $[M-2PF_6]^{2+}$: 1148.5661; found: 1148.5721.

3. The stability of lipid membranes upon addition of RT and RR[2]

3.1 Preparation LUVs \Rightarrow HPTS

To an EYPC solution (10 mg, 400 μ L, 25 mg/mL in $CHCl_3$) was added cholesterol (1 mg, 100 μ L, 10 mg/mL in $CHCl_3$). The obtained mixture was dried by a slow stream of nitrogen to evaporate the solvent through the needle tip and further dried in vacuum for 12 h. The lipid membrane was hydrated with 500 μ L HPTS-HEPES buffer (10 mM HEPES, 100 mM KCl, 1 mM HPTS, pH = 7.0) and stirred in a shaker for 2 h (37 $^{\circ}C$, 180 rad/min). The suspension was proceeded freeze-thaw cycles for 6 times with liquid nitrogen and warm water (-196 $^{\circ}C$ / 40 $^{\circ}C$), respectively, and extruded 21 times with a vesicle extruder equipped with a 100 nm polycarbonate membrane. The vesicle solution was purified by a size exclusion column (the padding material was SephadexTM G-25 and the mobile phase was HEPES buffer), and further diluted to 12.9 mL with HEPES buffer to afford vesicle stock solution with lipid concentration of 1.0 mM (assuming that all small phospholipid molecules were used to form vesicles).

3.2 Dynamic Light Scattering (DLS) analysis

According to the previously reported test method [1], 2900 μ L of HEPES buffer (100 mM KCl, 10 mM HEPES, pH = 7.0) was added to a quartz cuvette followed by addition of above 100 μ L of fresh LUVs \Rightarrow HPTS. Then, the samples with or without addition of **RT** and **RR[2]** (10 μ L DMSO with final concentration of 5.0 μ M) were analyzed by DLS.

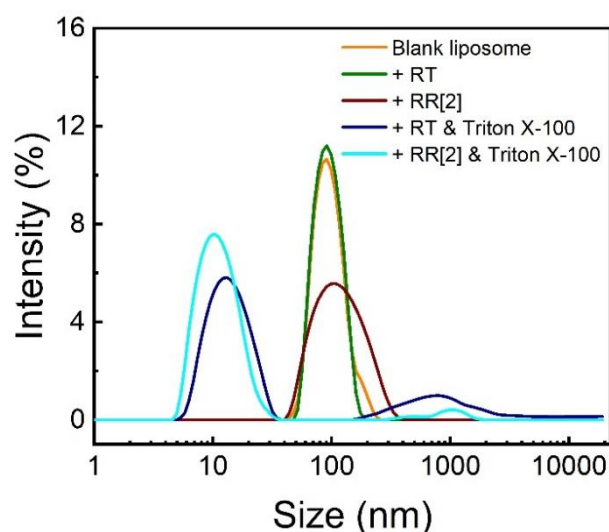


Fig. S1. DLS analysis of LUVs after the addition of **RT** and **RR[2]** (5.0 μM) in the absence and presence of surfactant Triton X-100 (5% aqueous solution). Blank liposome (LUVs \supset HPTS) was used as the control.

4. Ion transporting activity studies

4.1 Ion transport activity determined by LUVs \supset HPTS assay

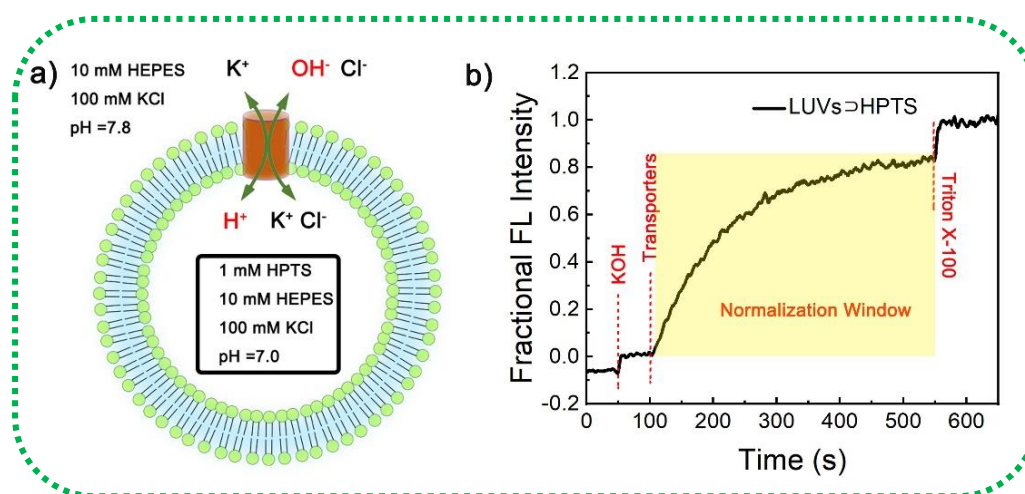


Fig. S2. a) Schematic illustration of fluorescence-based LUVs \supset HPTS assay and b) representative fluorescence kinetics experiment of ion transport.

The general process for LUVs \supset HPTS assay: In a typical experiment, to a HEPES buffer (2900 μL , 10 mM HEPES, 100 mM KCl, pH= 7.0) in a quartz cuvette was added 100 μL LUVs \supset HPTS (1.0 mM). Then, the cuvette was placed in a fluorescence spectrophotometer with stirring function, and the time-dependent change in fluorescence intensity ($\lambda_{\text{em}} = 510 \text{ nm}$) was monitored at two excitation wavelengths

simultaneously (I_{450} : λ_{ex} = 450 nm, I_{405} : λ_{ex} = 405 nm). During the experiments, KOH aqueous solution (30 μ L, 0.5 M, Δ pH= 0.8) was added at $t = 50$ s, compounds (10 μ L stock solution in DMSO, 0-5.0 μ M final concentration) was added at 100 s, and 5% Triton X-100 aqueous solution (60 μ L) was added at 550 s as the equilibrium end point. The temperature was kept at 25 $^{\circ}$ C by a stirrer and a temperature controller.

Data processing: Time courses of fluorescence intensity I_F were obtained by first, ratiometric analysis ($R= I_{450}/I_{405}$) and second, normalization according to Equation S1.

$$I_F = \frac{R-R_{100}}{R_{\infty}-R_{100}} \quad \text{Equation S1}$$

where R_{100} is R before addition of transporter and R_{∞} is the R after addition of Triton X-100. The effect of solvent DMSO (10 μ L) was also monitored and used as the fluorescence background. I_t at 550 s just before addition of Triton X-100 was defined as transmembrane activity Y ($Y= I_F- I_{DMSO}$). After analyzed with Hill Equation S2, EC_{50} values (the effective concentration required for 50% activity) and Hill coefficient n were obtained.

$$Y = Y_{\infty} + \frac{Y_0 - Y_{\infty}}{1 + \left(\frac{c}{EC_{50}}\right)^n} \quad \text{Equation S2}$$

Where Y_0 is Y in absence of transporter (normally defined as 0), Y_{∞} is Y with excess transporter (normally defined as 1) and c is the transporter concentration.

For clarity, the data before the addition of transporter was deleted and time (X-axis) was changed to start from the point of transporter addition (i.e. $t = 100$ s was normalized to $t = 0$ s) to the end point of experiment (i.e. $t = 550$ s was normalized to $t = 450$ s), as shown in the yellow window of Figure S2b).

Data analysis: All the data in LUVs assays were averaged from three repeated experiments, and showed as mean \pm SEM. Significant differences analysis is conducted for those comparative data with small differences.

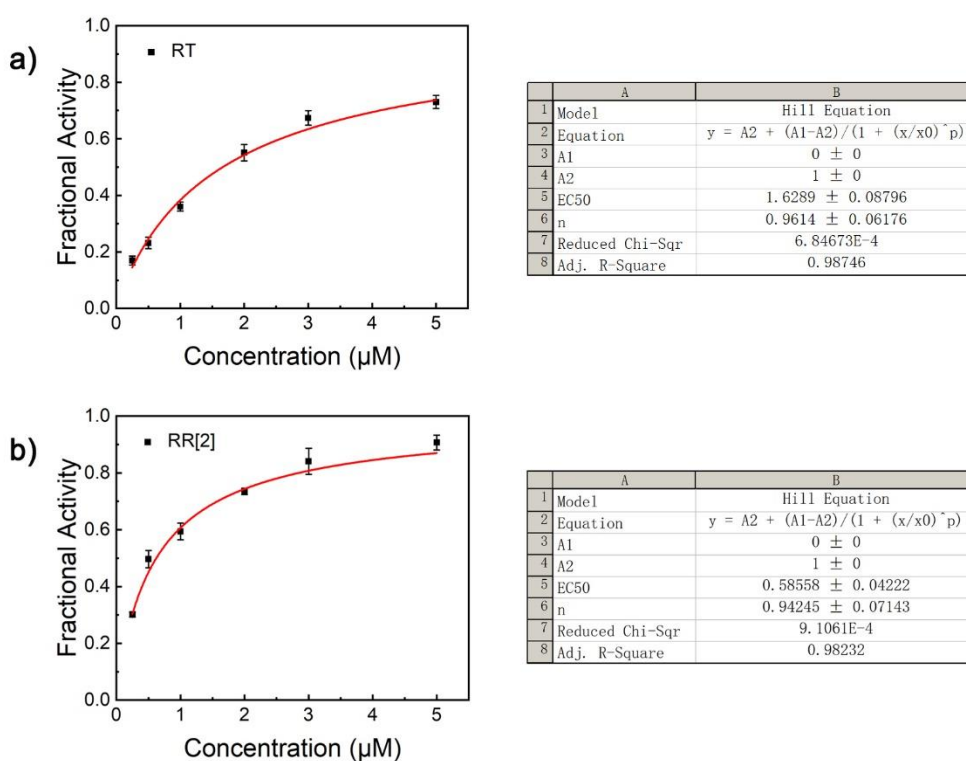


Fig. S3. Hill analysis for the dosage-response curves of a) **RT** and b) **RR[2]** in LUVs⊃HPTS assay, in which EC₅₀ value can be obtained. The selected concentrations of compounds are at 0, 0.25, 0.5, 1.0, 2.0, 3.0, 5.0 μM, respectively.

Table 1 The summarized data from Hill analysis.

	EC ₅₀ (μM)	n	Adj.R-Square
RT	1.62 ± 0.087	0.96 ± 0.062	0.98232
RR[2]	0.58 ± 0.042	0.94 ± 0.071	0.98746

4.2 The importance of rotaxane activity structure.

The procedure was similar as that of above LUVs⊃HPTS assay, except B18C6 in DMSO (final concentration 1.0 μM) was added at 75 s. The data analysis was in the same way as stated above (in section 4.1). The results showed that the addition of B18C6 would increase the activity of RT, but this effect was only an independent additive relationship. However, when they were combined into a rotaxane structure, the much higher activity indicated the synergistic effect on ion transport.

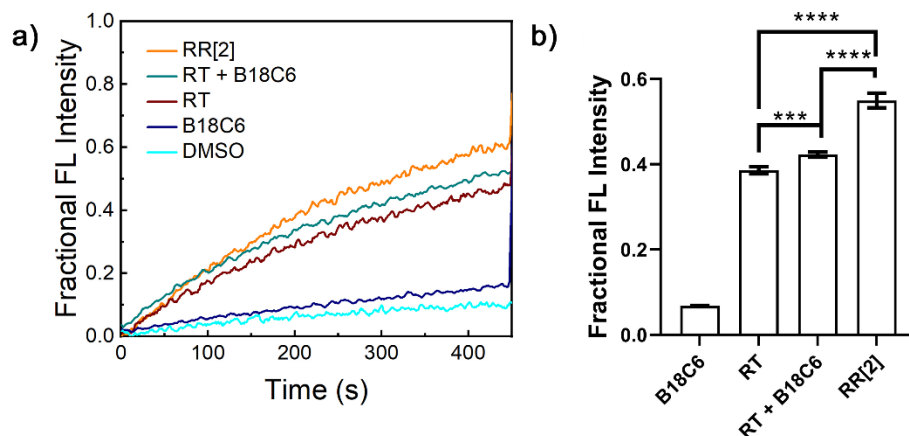


Fig. S4. a) Activity comparison for **RT** (1.0 μM) in presence and absence of **B18C6** (1.0 μM) and the comparison with **RR[2]** (1.0 μM) using LUVs \Rightarrow HPTS assay, and b) column histogram of activity comparison from a), *** means $p < 0.001$; **** means $P < 0.0001$.

4.3 DPX membrane-leakage analysis

In a typical experiment, 100 μL of above stocked LUVs \Rightarrow HPTS solution (1.0 mM) and 2900 μL of HEPES buffer (10 mM HEPES, 100 mM KCl, pH = 7.0) were mixed in a quartz cuvette. Then, compounds **RT** and **RR[2]** (10 μL stock solutions in DMSO, the final concentrations are 5.0 μM , respectively) was added and stirred for 10 min. Subsequently, p-xylene-bis-pyridinium bromide (DPX) quencher (1.0 mM) was added and the fluorescent excitation spectra were explored (emission at 510 nm). Meanwhile, detergent Triton X-100 (5% aqueous solution) was added and the sample was used as the negative control.

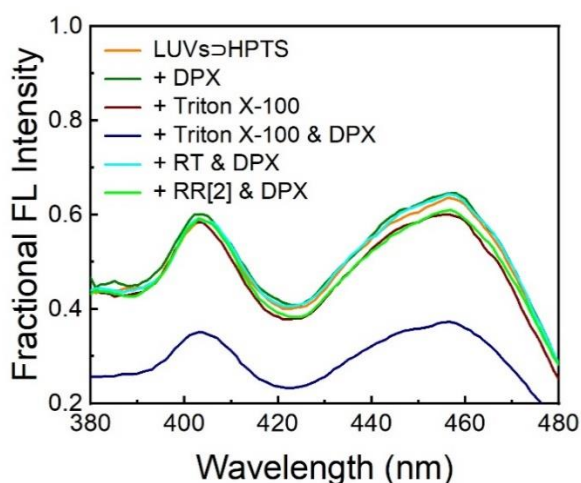


Fig. S5. Fluorescence excitation spectra of DPX quenching assay with $\lambda_{\text{em}}=510$ nm.

4.4 Ion transport rates

The activity (Y) was interactively fitted by a first-order exponential decay equation (Equation S3), in which the observed first-order rate constants k_{obs} were obtained.

$$Y = Y_0 (1 - e^{-k_{obs}t}) \quad \text{Equation S3}$$

The dependence of the observed rate (k_{obs}) on the concentration of transporters can be used to determine the aggregation state of the channel, or the number of monomers that form the active structure (Equation S4).

$$k_{obs} \propto [\text{monomer}]^n \quad \text{Equation S4}$$

If the k_{obs} showed a linear increase with concentrations, it was indicative of monomolecular active structure for ion transport. To avoid the adverse effects of possible precipitation of compounds, the transport rates k_{obs} were calculated from the data in low concentrations.

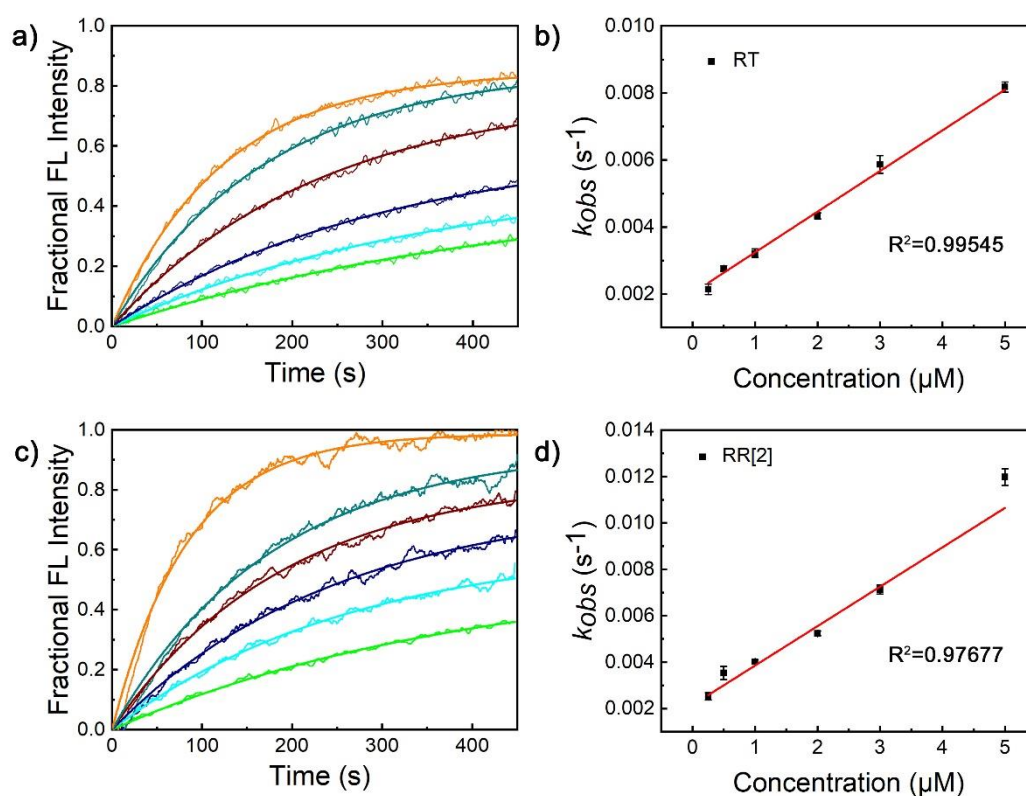


Fig. S6. Plots of k_{obs} against concentrations of a-b) RT (0.25-5.0 μM) and c-d) RR[2] (0.25-5.0 μM). a) and c) are the representative one group of data for k_{obs} fitting by a first-order exponential decay equation, b) and d) are the fitting treatments for linear relationship between k_{obs} and concentrations.

4.5 Ion selectivity studies across LUVs \supset HPTS

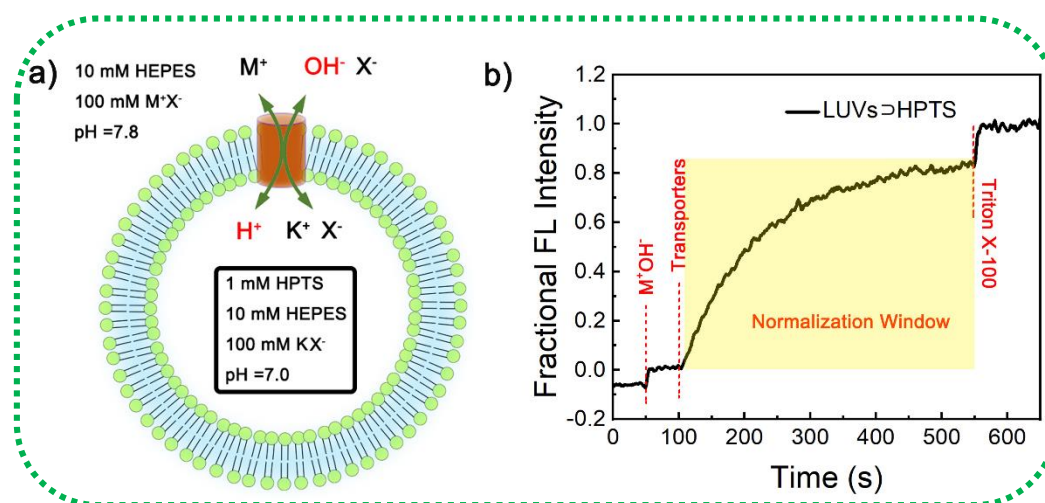


Fig. S7. a) Schematic illustration of ion selectivity assay using LUVs \supset HPTS and b) representative fluorescence kinetics experiment of ion transport.

Cation selectivity determined by LUVs \supset HPTS assay: The process for cation selectivity was similar to that of activity investigation by LUVs \supset HPTS assay, except different HEPES buffer solutions (10 mM HEPES, 100 mM MCl, pH = 7.0; where, M⁺ = Li⁺, Na⁺, K⁺, Rb⁺ and Cs⁺) were used as the dilute solution (2900 μ L) and different bases (30 μ L, 0.5 M MOH, M⁺ = Li⁺, Na⁺, K⁺, Rb⁺ and Cs⁺) were added to generate pH gradient. The data processing was in the same way as for the normal LUVs \supset HPTS assay.

Anion selectivity determined by LUVs \supset HPTS assay: The process for anion selectivity was similar to that of activity investigation by LUVs \supset HPTS assay, except different HEPES buffer solutions containing different anions (10 mM HEPES, 100 mM KX, pH = 7.0, X⁻ = Cl⁻, Br⁻, I⁻, NO₃⁻, SO₄²⁻) were used as both the extra- and intravesicular solutions. The data processing was in the same way as for the normal LUVs \supset HPTS assay.

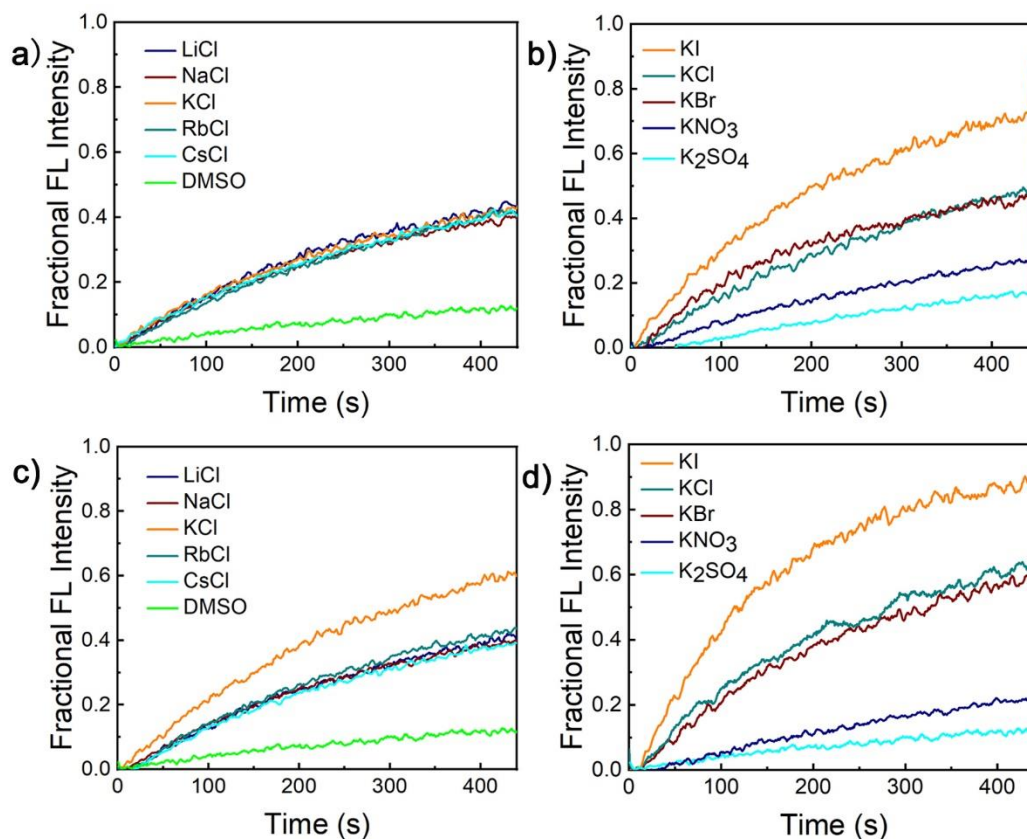


Fig. S8. a) Cation selectivity and b) anion selectivity of **RT** at 1.0 μM . c) Cation selectivity and d) anion selectivity of **RR[2]** at 1.0 μM .

4.6 Complementary LUVs \Rightarrow HPTS assay

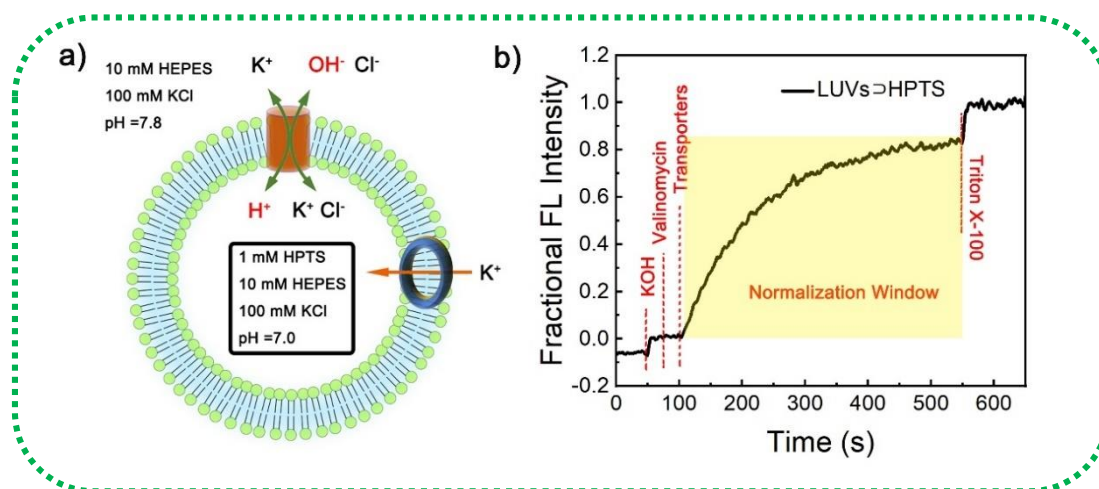


Fig. S9. Schematic illustration of Valinomycin assay using LUVs \Rightarrow HPTS a) and representative fluorescence kinetics experiment of ion transport b).

Valinomycin assay: The procedure for the valinomycin complementary test was similar as that of routine LUVs \Rightarrow HPTS assay, except valinomycin in DMSO (final concentration 0.1 μM) was added at 75 s. The data analysis was in the same way as

stated above (in section 4.1).

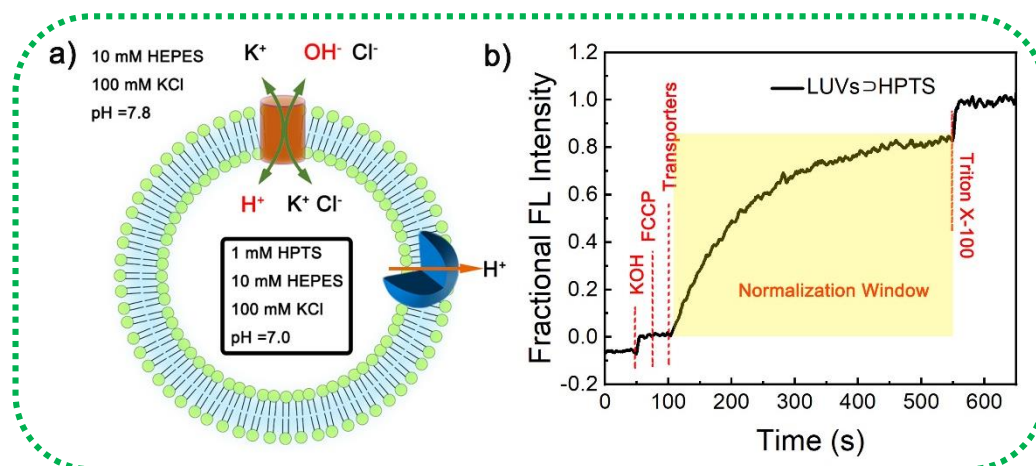


Fig. S10. Schematic illustration of FCCP assay using LUVs \Rightarrow HPTS a) and representative fluorescence kinetics experiment of ion transport b).

FCCP assay: The procedure for the valinomycin complementary test was similar as that of routine LUVs \Rightarrow HPTS assay, except FCCP in DMSO (final concentration 0.01 μ M) was added at 75 s. The data analysis was in the same way as stated above (in section 4.1).

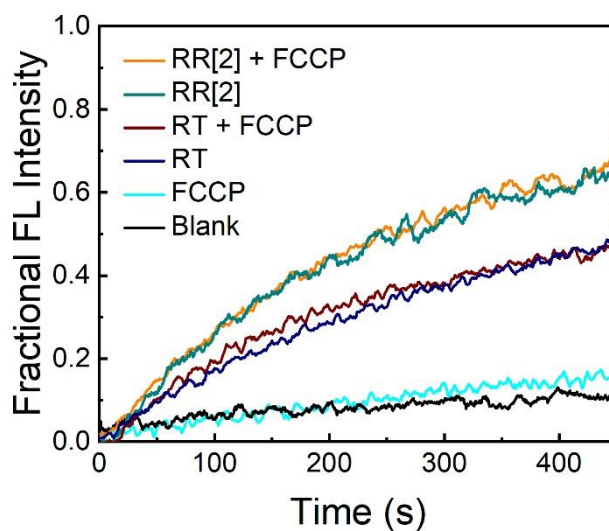


Fig. S11. Comparison of transport activity in presence and absence of FCCP (0.01 μ M) for RT and RR[2] at 1.0 μ M.

5. LUVs \Rightarrow lucigenin assay for Cl^- transport

5.1 Preparation of LUVs \Rightarrow lucigenin

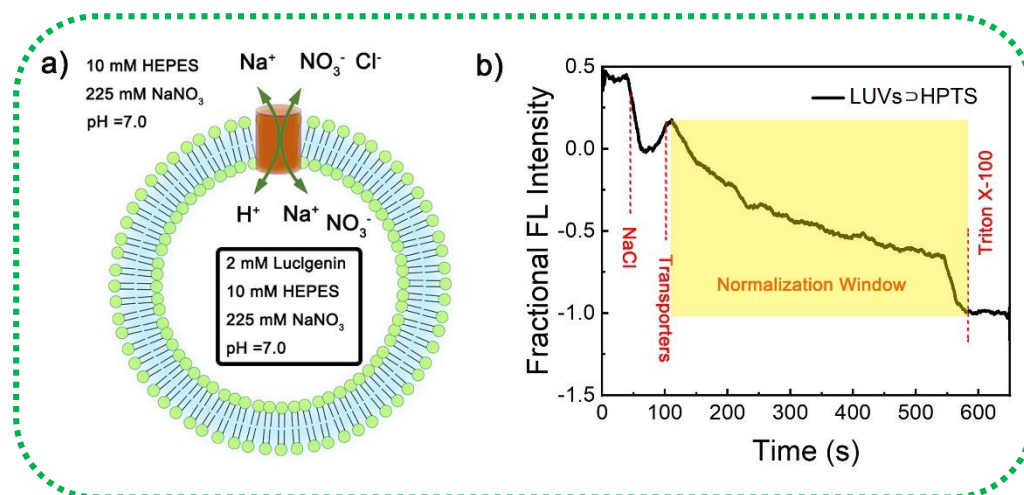


Fig. S12. Schematic illustration of chloride influx assay using LUVs⊃lucigenin a) and representative fluorescence kinetics experiment of corresponding assay b).

LUVs⊃lucigenin vesicles were prepared similar to the LUVs⊃HPTS (section 3.1), except a buffer contained 10 mM HEPES, 225 mM NaNO₃, 2.0 mM N, N'-dimethyl-9,9'-biacridinium dinitrate (lucigenin) (pH = 7.0) was used for hydration. The obtained vesicle suspension was purified with size exclusion column chromatography (Sephadex G-25) and further diluted with HEPES buffer (10 mM HEPES, 225 mM NaNO₃, pH = 7.0) to obtain LUVs⊃lucigenin stock solution with total lipid concentration of 1.0 mM.

5.2 LUVs⊃lucigenin assay

The general process for LUVs⊃lucigenin assay: In a clean and dry fluorescence cuvette, 100 μL of above lipid solution and 2900 μL of 225 mM NaNO₃ HEPES solution was taken and kept in slowly stirring condition by a magnetic stirrer equipped with the fluorescence instrument (at t = 0 s). In this assay, the time course of lucigenin fluorescence emission intensity R was observed at λ_{em} = 535 nm (λ_{ex} = 450 nm). 30 μL of 3.0 M NaCl was added to the cuvette at t = 50 s to make salt gradient between the intra and extra vesicular system. Transporters was added at t = 100 s, and finally at t = 550 s, 60 μL of 5% Triton X-100 was added to lyse the vesicles for 100% chloride influx.

Data processing: The data analysis was collected in the yellow widow (Fig. S12b). Fluorescence intensities were normalized to fractional emission intensity I_F using

Equation S5.

$$I_F = \frac{R - R_{100}}{R_{\infty} - R_{100}} \times (-100\%) \quad \text{Equation S5}$$

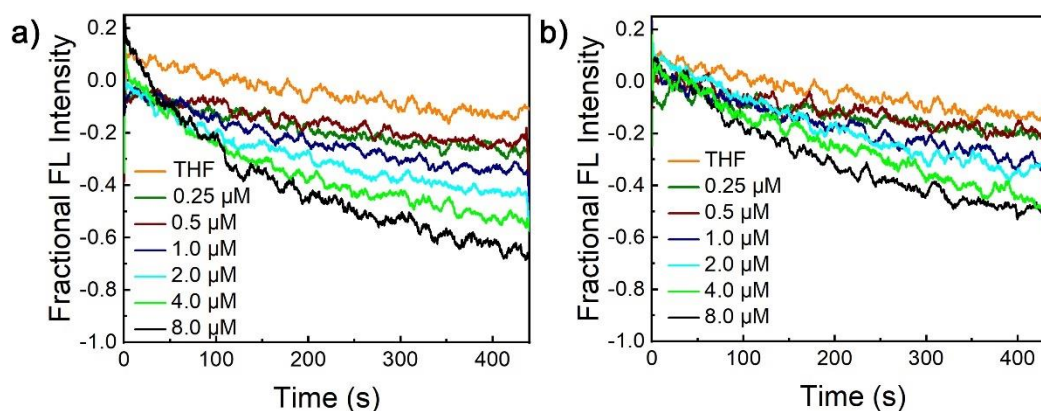


Fig. S13. Cl^- ion influx across LUVs \supset lucigenin assay upon addition of RT (0-8.0 μM) and RR[2] (0-8.0 μM).

5.3 LUVs \supset lucigenin assay with Na_2SO_4

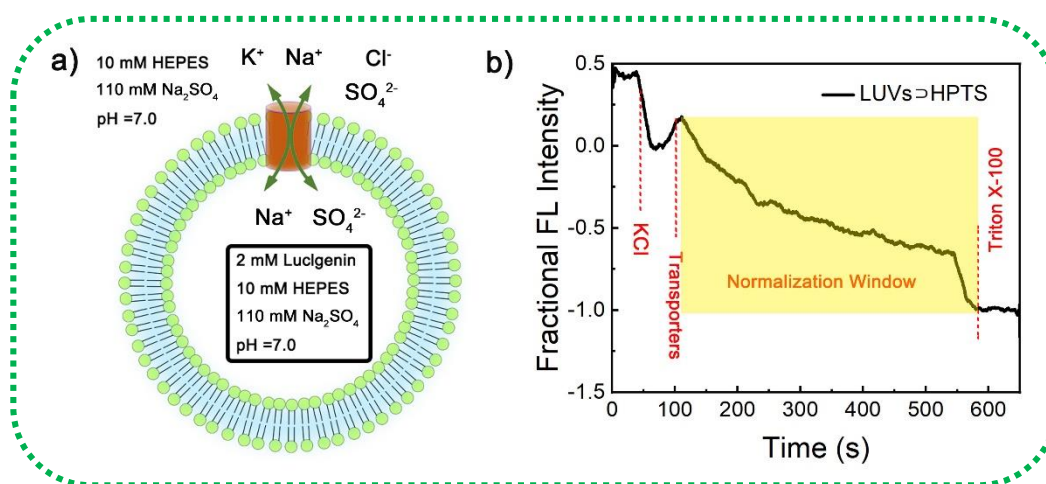


Fig. S14. a) Schematic illustration of chloride influx assay using LUVs \supset lucigenin with Na_2SO_4 solution and b) representative fluorescence kinetics experiment of corresponding assay.

LUVs \supset lucigenin vesicles were prepared similar to the LUVs \supset HPTS (section 3.1), except a buffer contained 10 mM HEPES, 110 mM Na_2SO_4 , 2.0 mM N,N'-dimethyl-9,9'-biacridinium dinitrate (lucigenin) (pH = 7.0) was used for hydration. The obtained vesicle suspension was purified with size exclusion column chromatography (Sephadex G-25) and further diluted with HEPES buffer (10 mM HEPES, 110 mM Na_2SO_4 , pH =

7.0) to obtain LUVs Δ lucigenin stock solution with total lipid concentration of 1.0 mM. The experimental procedure and data analysis was similar as the general LUVs Δ lucigenin assay, except that KCl was used to make salt gradient.

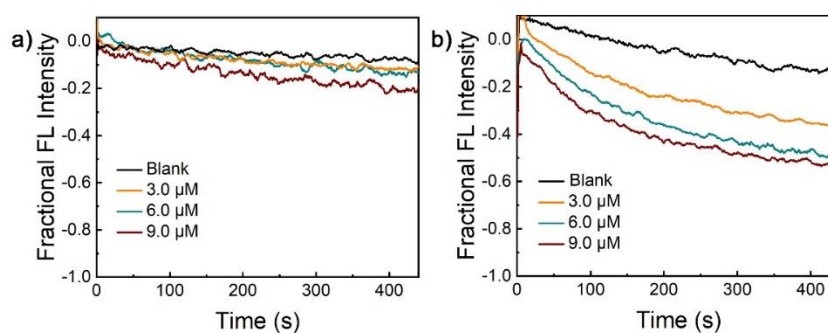


Fig. S15. Cl⁻ ion influx across LUVs Δ lucigenin assay (Na₂SO₄ was used to replace intra- and extra-vesicular NaNO₃) upon addition of a) **RT** (0-9.0 μ M) and b) **RR[2]** (0-9.0 μ M).

6. Planar Bilayer Conductance Measurements

6.1 General experiments for RT and RR[2]

General process: A CDCl₃ solution of 1,2-diphytanoyl-sn-glycero-3-phosphocholine (DPhPC) was evaporated using a stream of nitrogen. After keeping under high vacuum for 4 h, the obtained film was dissolved in n-decane with a concentration at 20 mg mL⁻¹. The obtained solution was used to precoat a 200 μ m hole of a polystyrene cup held by a chamber upon which a planar lipid bilayer membrane was formed. For general conductance investigation, the cup (cis) and chamber (trans) were filled with 1.0 mL 1.0 M KCl solution. The Ag-AgCl electrodes were placed into the two solutions with the trans side grounded. The formation of planar lipid bilayer was confirmed by measuring membrane capacitance value with the output value around 80-120 pF (the formation of a single bilayer of phospholipid membrane). Channel molecules (10 μ L stock solution in DMSO with 3.0 μ M final concentration) was added to the cis side of the chamber. Various holding potentials were applied and the channel responses were recorded. The Ag-AgCl electrodes were used to inject current and detect the current signal caused by ion transport. The entire experimental process was

completed on an Axon patch clamp workstation. The currents were measured by a Warner BC-535 bilayer clamp amplifier and collected using the Digidata 1550A data acquisition system. All data was filtered with 8-pole Bessel filter, stored by Clampex software (version 10.0; Axon Instruments, Foster City, CA), and finally passed through Origin Lab 9.0 (Origin Lab Corporation, Northampton, MA, USA).

Data analysis: All the data in LUVs assays were averaged from three repeated experiments, and showed as mean \pm SEM. Significant differences analysis is conducted for those comparative data with small differences.

For **RT** molecules, we selected six different voltages of 50 mV, 100 mV, 150 mV, -50 mV, -100 mV, and -150 mV for testing. For **RR[2]**, 50 mV, 100 mV, 120 mV, -50 mV, -100 mV, -120 mV were selected. (The selected voltage has no special purpose and at least three signals per group of voltages were collected).

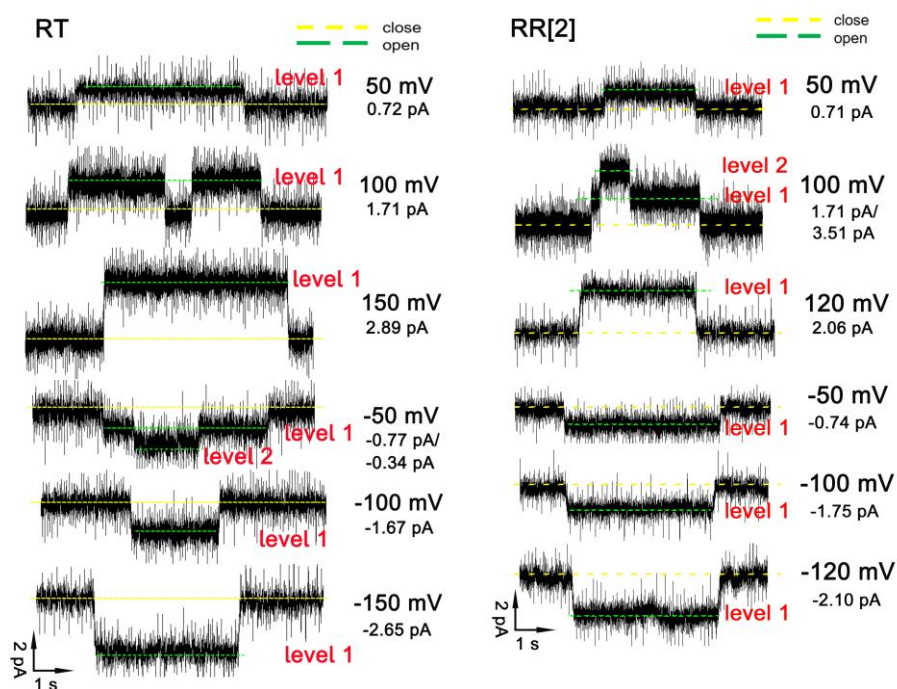


Fig. S16. Representative current recording of **RT** and **RR[2]** (3.0 μ M) at various holding potentials with symmetric KCl solution in both sides (1.0 M), which were used for determining conductance.

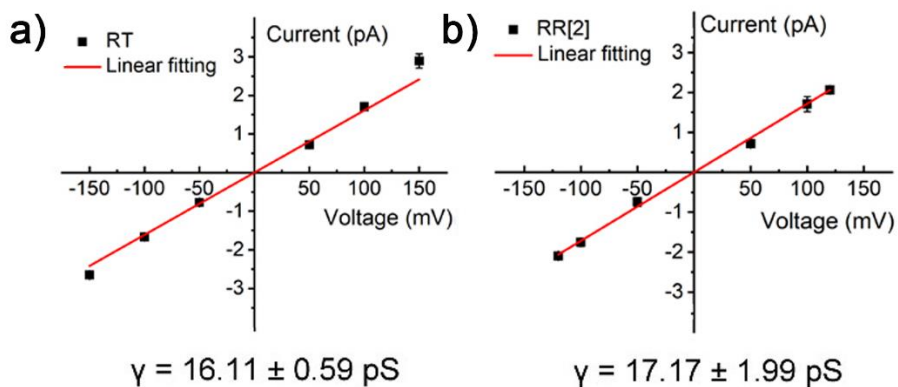


Fig. S17. Linear I-V plots of c) **RT** and d) **RR[2]** at 3.0 μM . The data was summarized from Figure S16.

6.2 Determination of $P_{\text{K}^+}/P_{\text{Cl}^-}$

For reversal potential investigation, the cup (cis, ground) and chamber (trans) were filled with 1 mL 0.5 M and 1.0 M KCl solution, respectively. Compounds **RT** or **RR[2]** in DMSO were added to the cis compartment to reach a final concentration of 3.0 μM . The selectivity of **RT** and **RR[2]** for K^+ over Cl^- , defined as the permeability ratio of two ions, was calculated by using Goldman-Hodgkin-Katz (GHK) equation:

$$\varepsilon_{rev} = \frac{RT}{F} \times \ln \frac{\sum P_M[M^+]_{cis} + \sum P_A[A^-]_{trans}}{\sum P_M[M^+]_{trans} + \sum P_A[A^-]_{cis}} \quad \text{Equation S6}$$

Where, ε_{rev} is the reversal potential, R is universal gas constant ($8.314 \text{ J K}^{-1} \text{ mol}^{-1}$), T is the temperature in Kelvin (300 K), F is the Faraday's constant (96485 C mol^{-1}). P is the permeability of **RT** or **RR[2]** for ions.

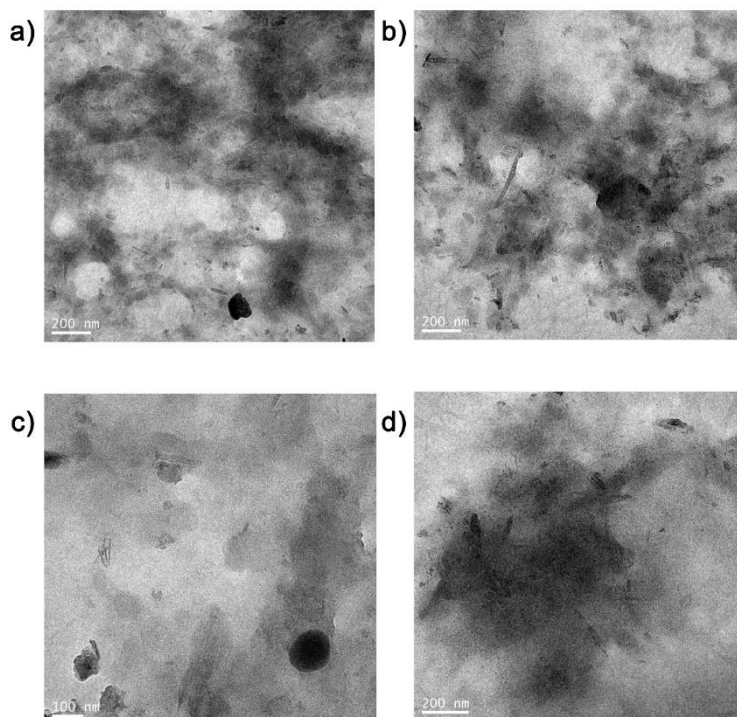


Fig. S19. a-d) TEM images of **RT** prepared from MeCN solution (2.5 mM).

8. Appendix: ^1H NMR, ^{13}C NMR and LC-MS Spectra for New Compounds

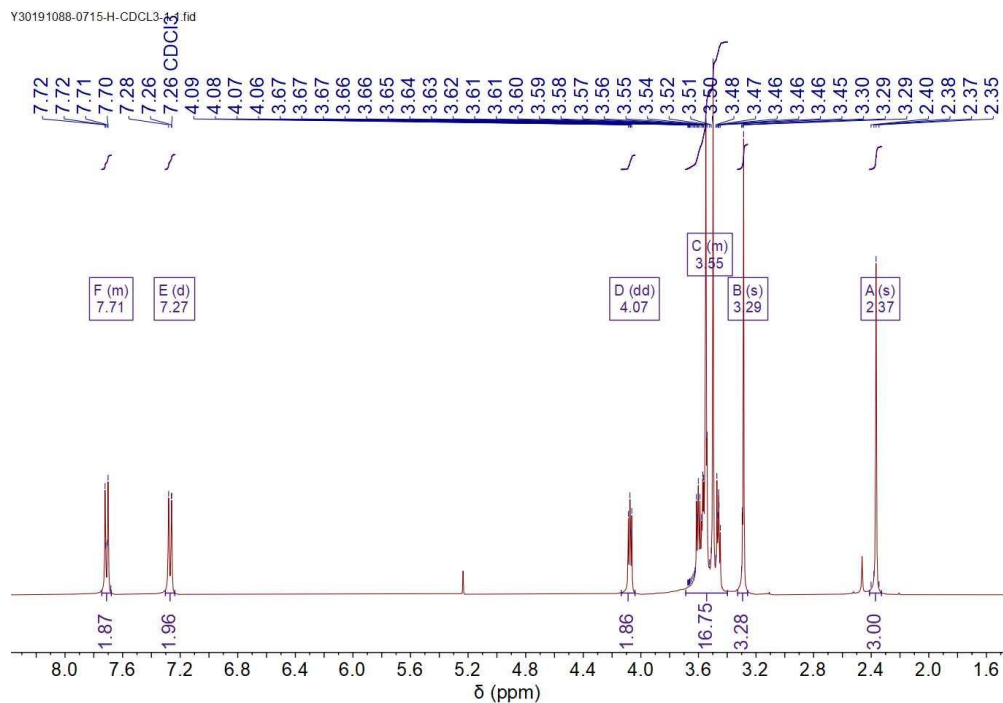


Fig. S20. ^1H NMR spectrum (400 MHz, CDCl_3-d_1) of A1.

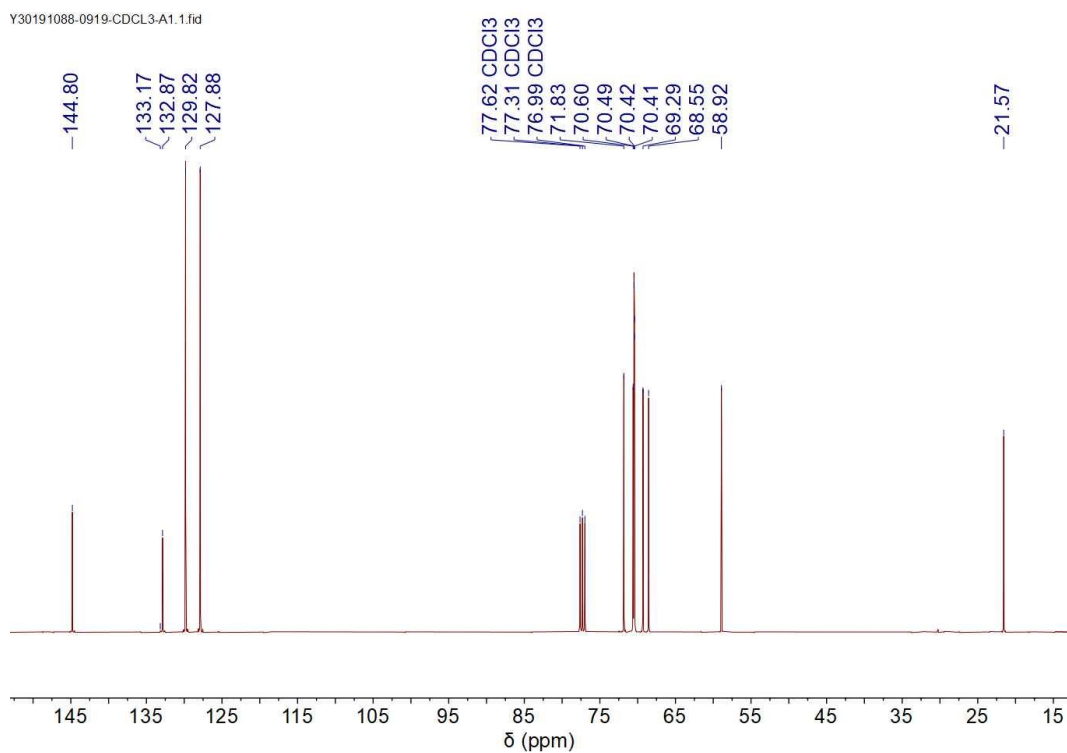


Fig. S21. ^{13}C NMR spectrum (101 MHz, CDCl_3-d_1) of A1.

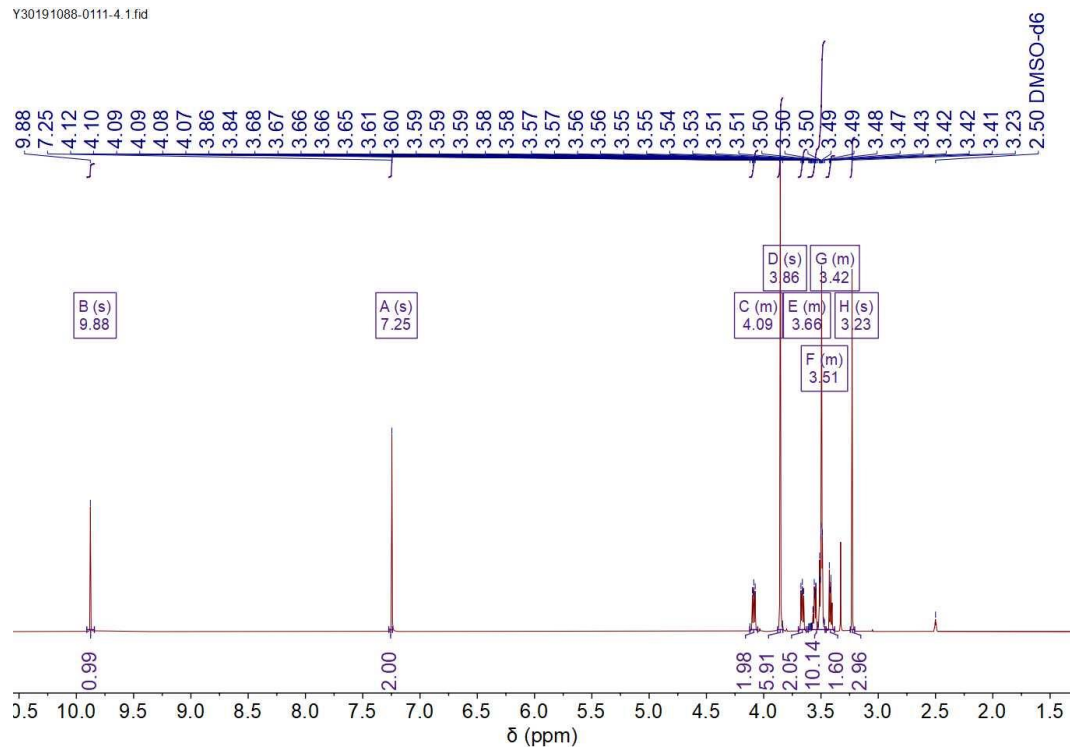


Fig. S22. ^1H NMR spectrum (400 MHz, $\text{DMSO-}d_6$) of A2.

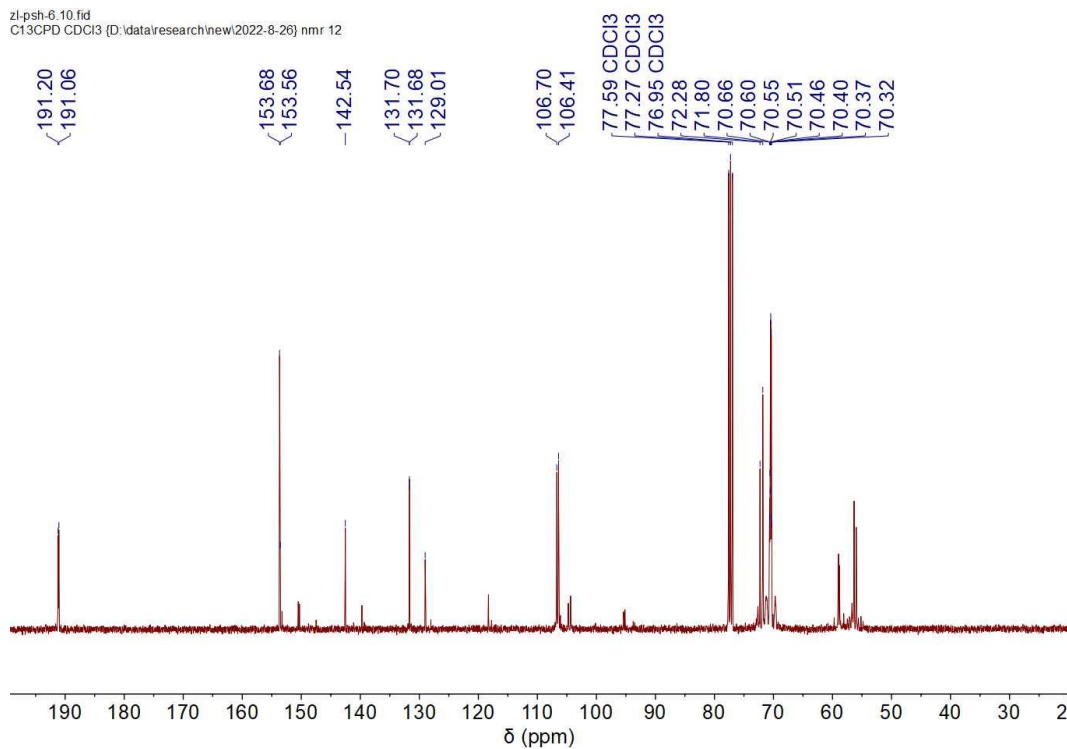


Fig. S23. ^{13}C NMR spectrum (101 MHz, CDCl_3-d_1) of A2.

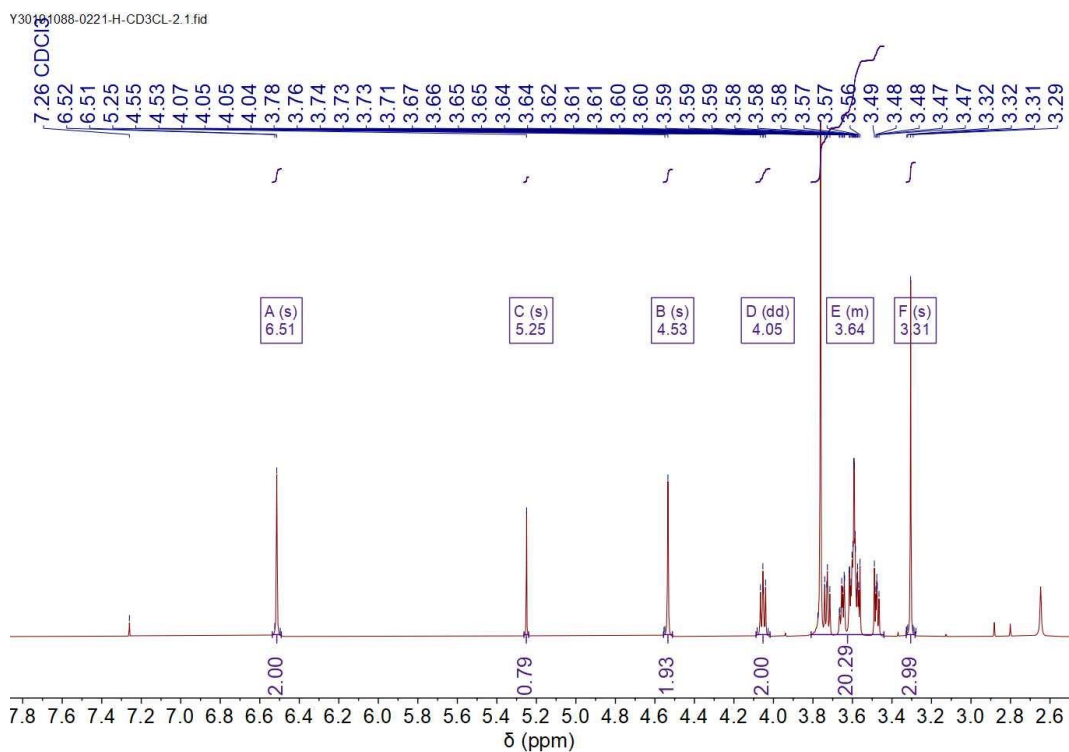


Fig. S24. ¹H NMR spectrum (400 MHz, CDCl₃-d₁) of A3.

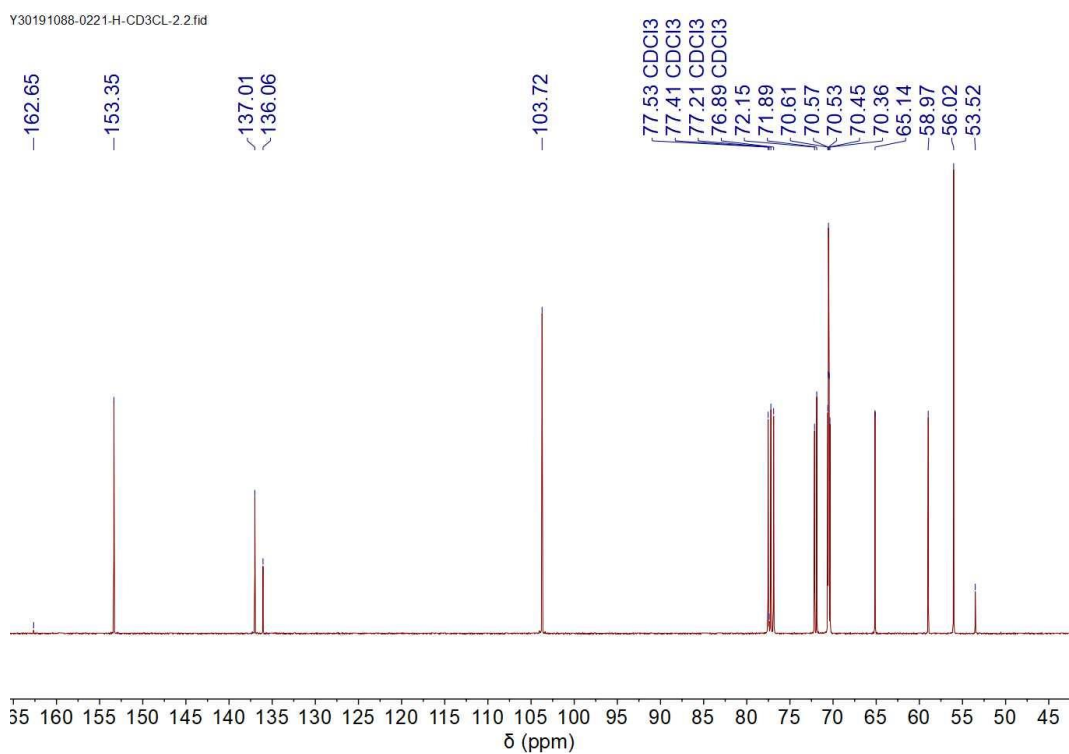


Fig. S25. ¹³C NMR spectrum (101 MHz, CDCl₃-d₁) of A3.

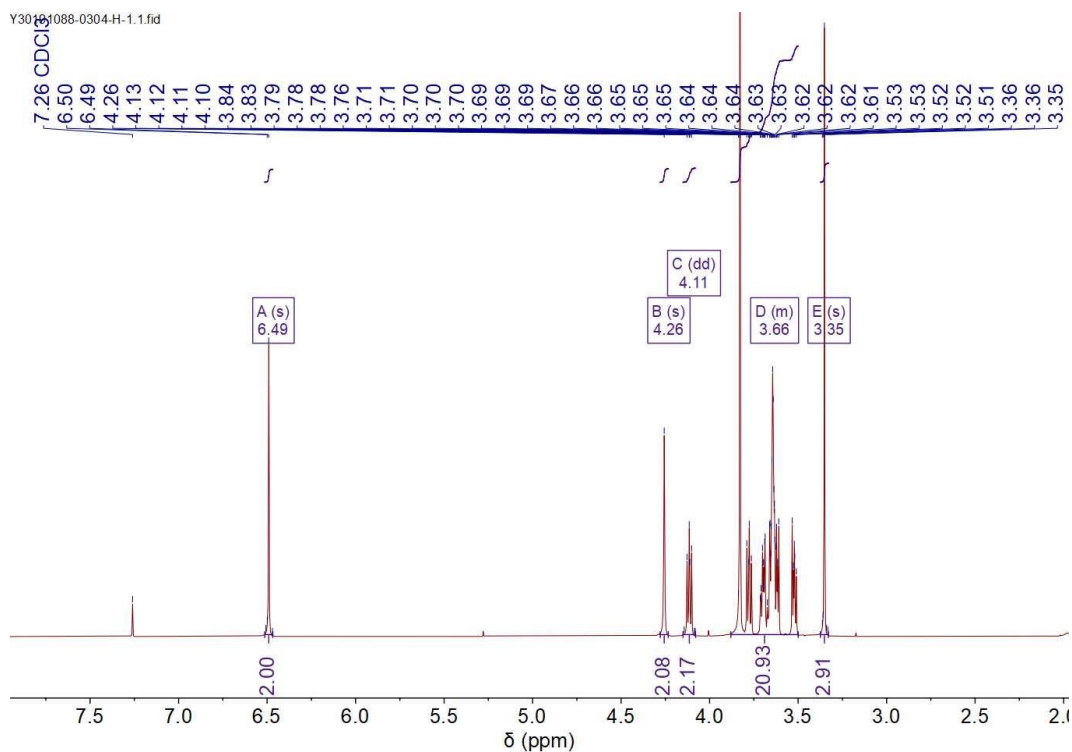


Fig. S26. ¹H NMR spectrum (400 MHz, CDCl₃-d₁) of A4.

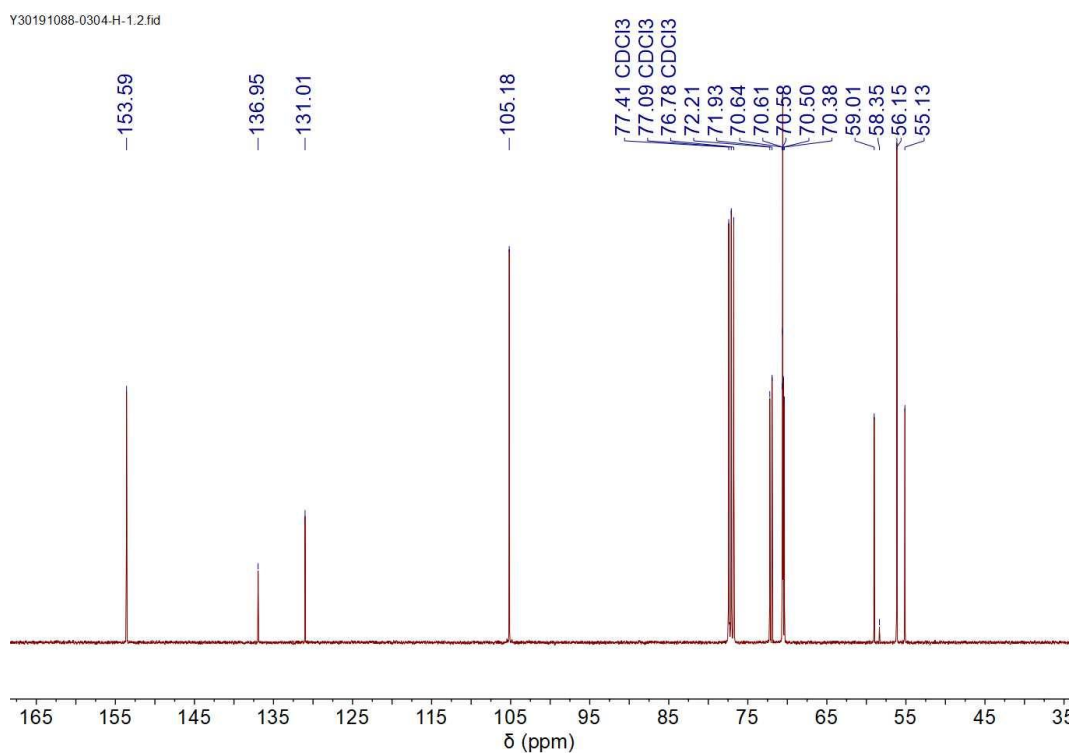


Fig. S27. ¹³C NMR spectrum (101 MHz, CDCl₃-d₁) of A4.

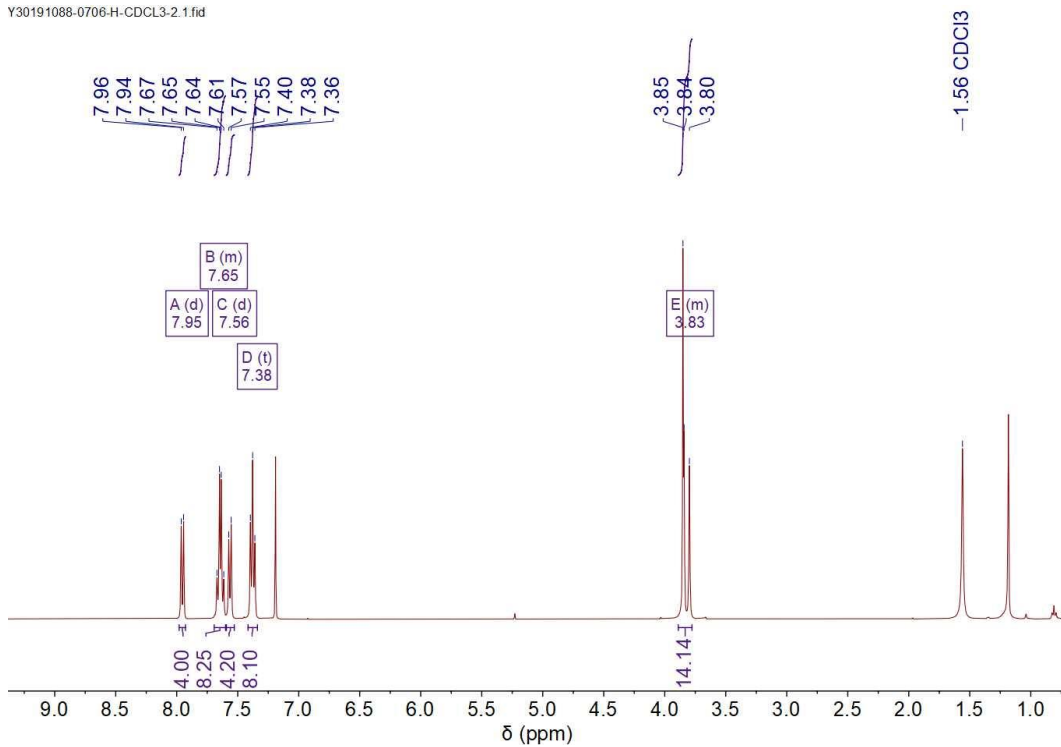


Fig. S28. ¹H NMR spectrum (400 MHz, CDCl₃-*d*₁) of B1.

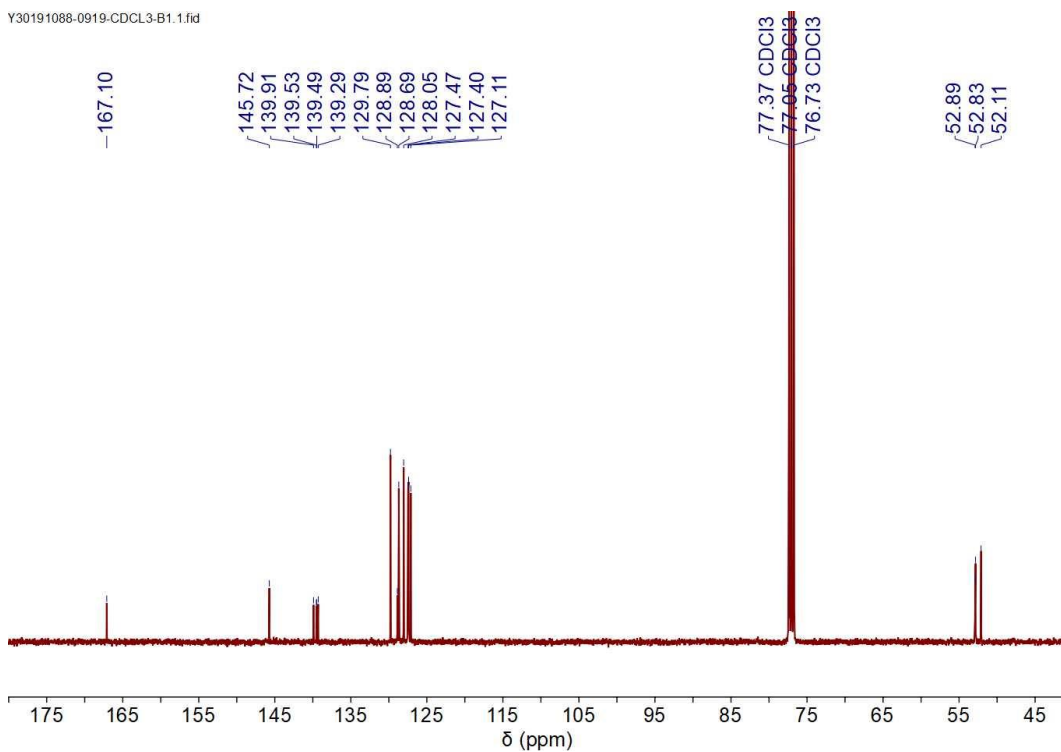


Fig. S29. ¹³C NMR spectrum (101 MHz, CDCl₃-*d*₁) of B1.

Y30191088-0711-H-3.1.fid

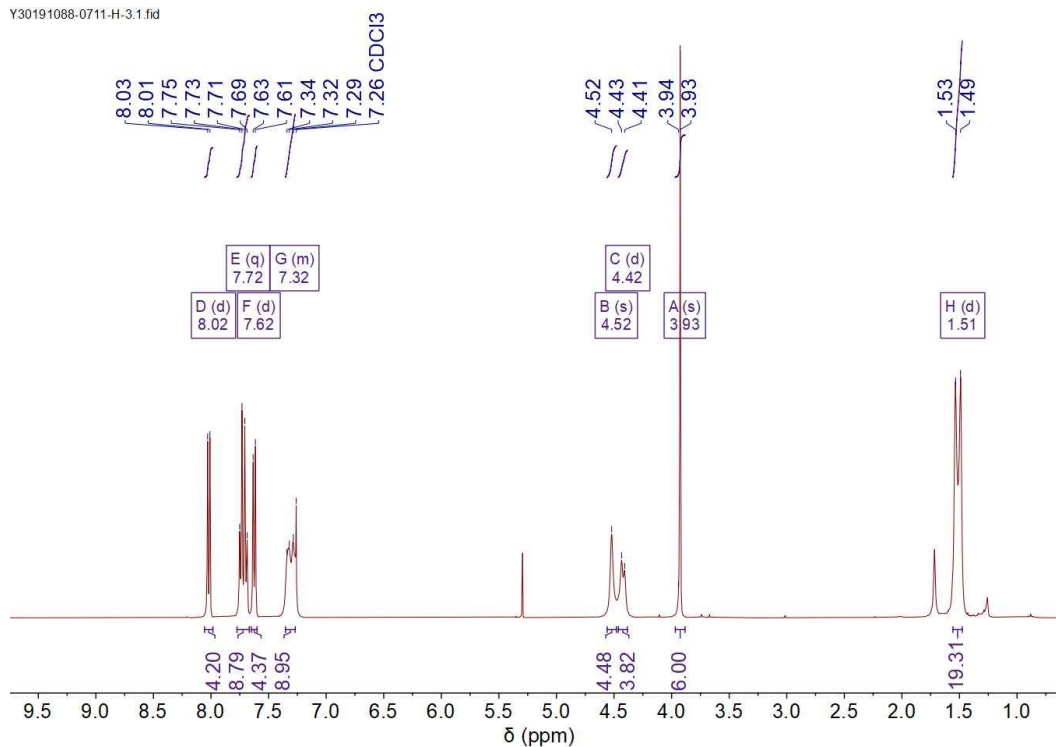


Fig. S30. ¹H NMR spectrum (400 MHz, CDCl₃-d₁) of B2.

Y30191088-0916-B2.1.fid

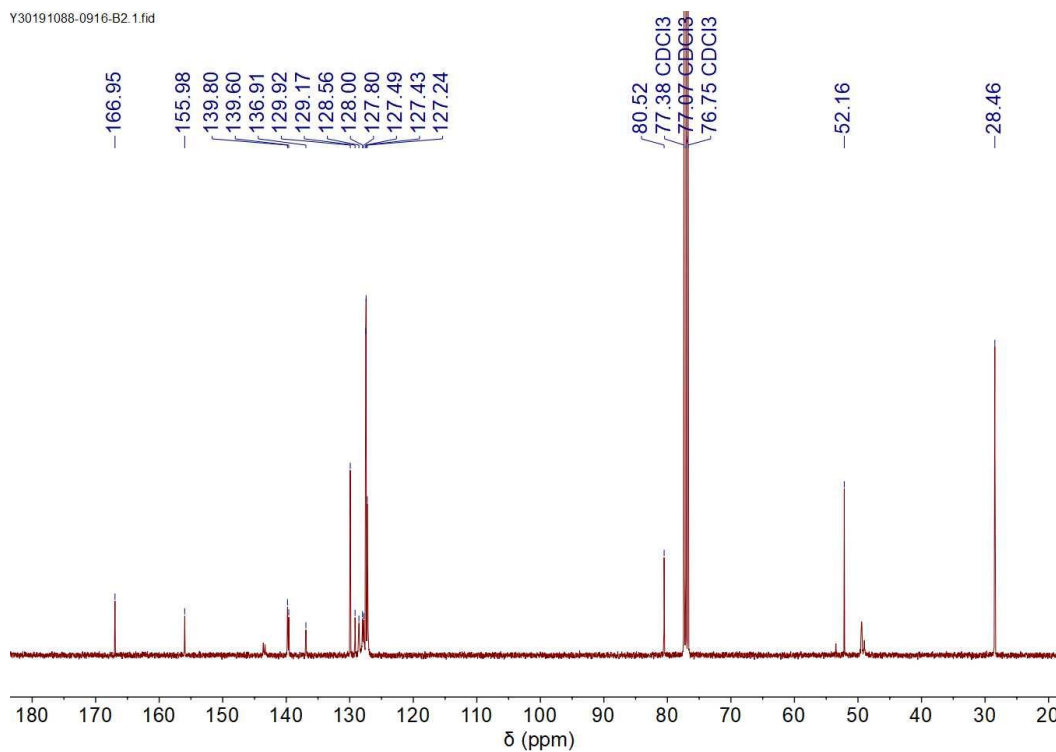


Fig. S31. ¹³C NMR spectrum (101 MHz, CDCl₃-d₁) of B2.

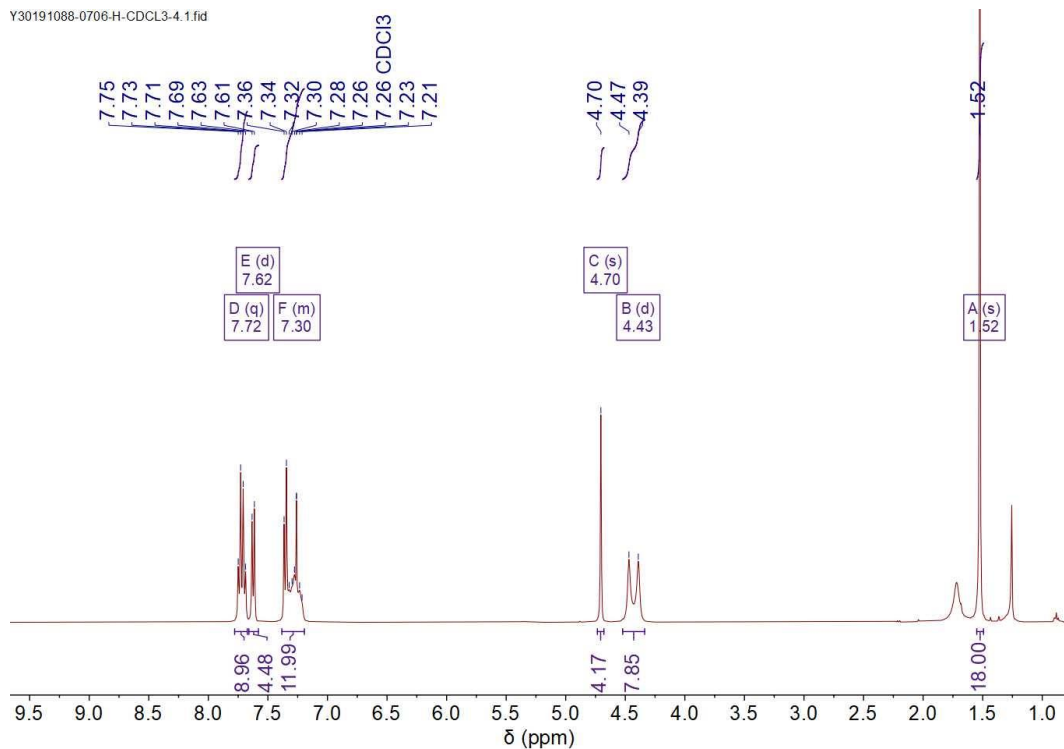


Fig. S32. ^1H NMR spectrum (400 MHz, CDCl_3-d_1) of B3.

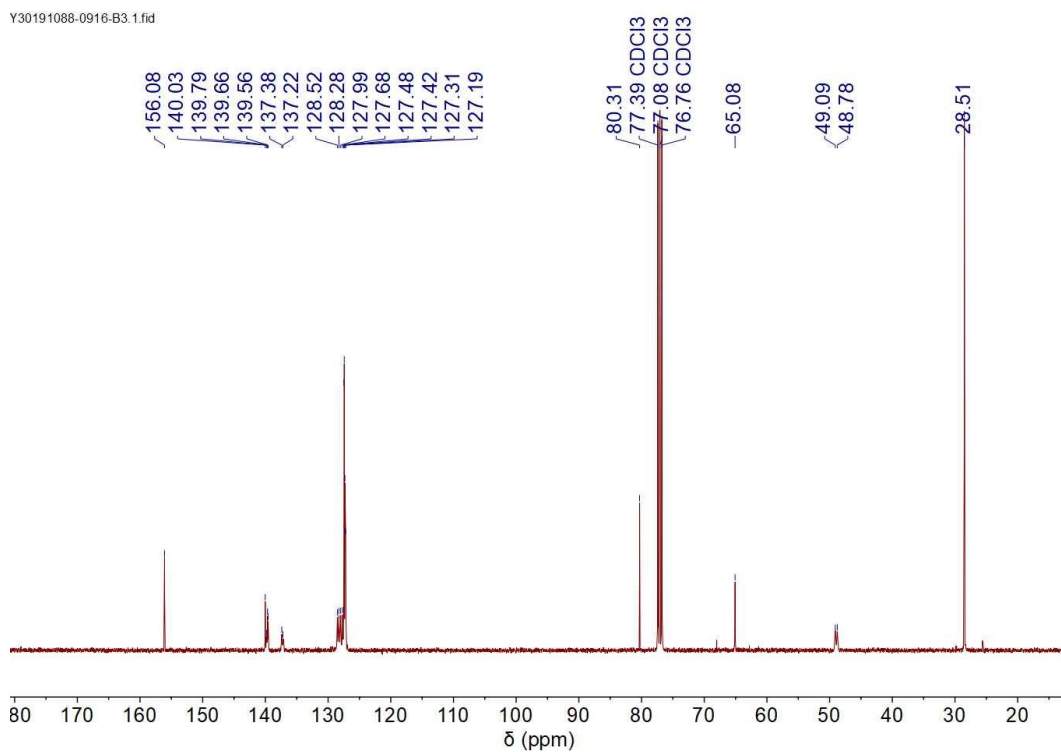


Fig. S33. ^{13}C NMR spectrum (101 MHz, CDCl_3-d_1) of B3.

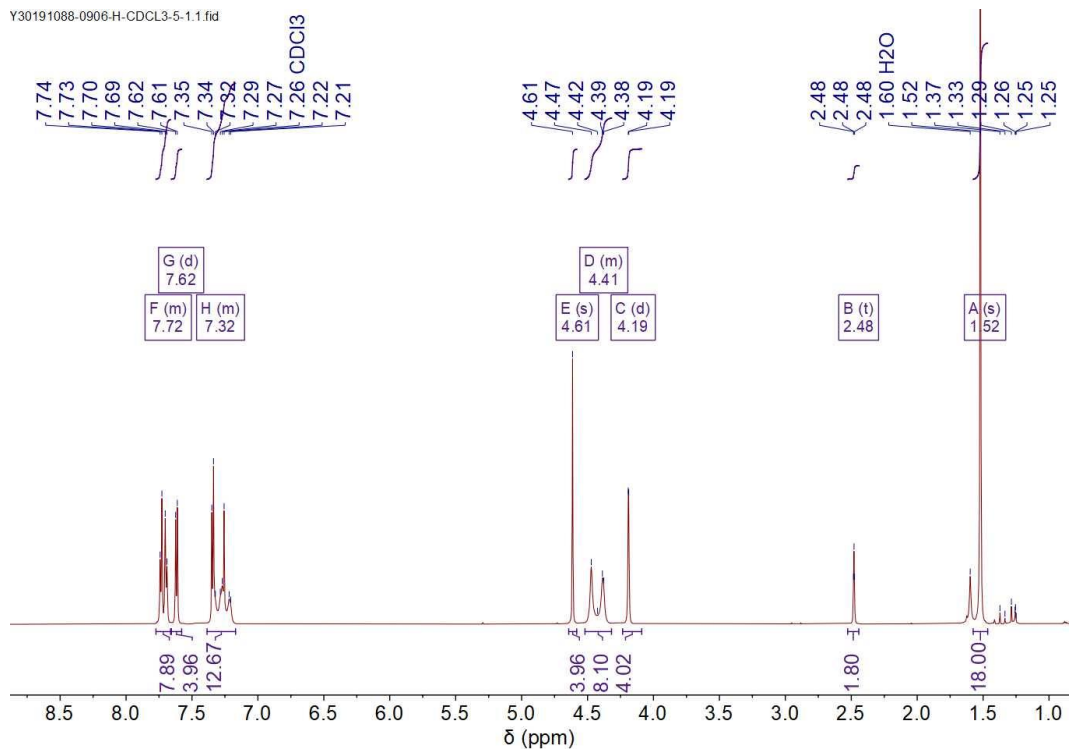


Fig. S34. ^1H NMR spectrum (400 MHz, CDCl_3-d_1) of B4.

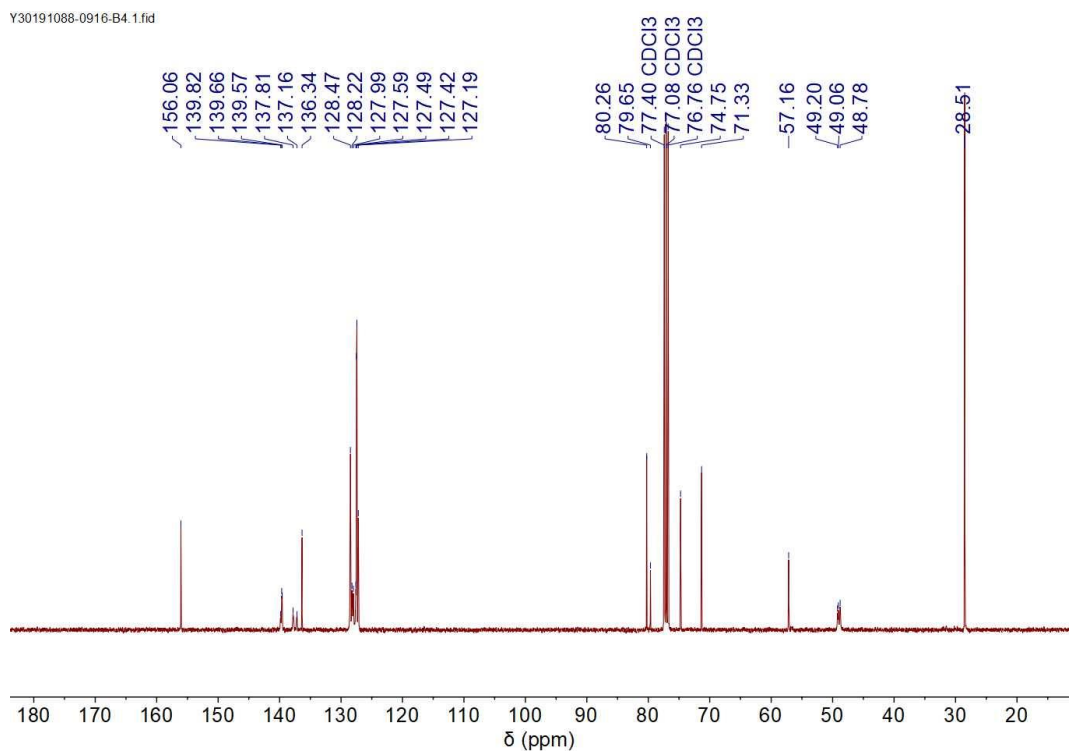


Fig. S35. ^{13}C NMR spectrum (101 MHz, CDCl_3-d_1) of B4.

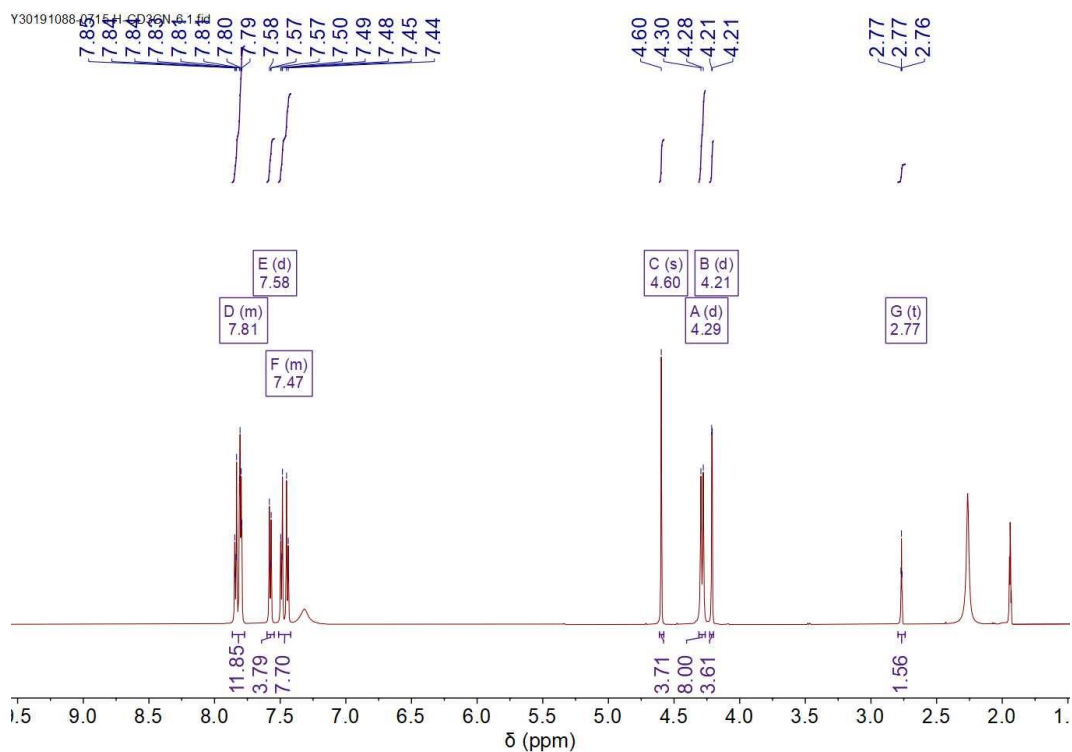


Fig. S36. ^1H NMR spectrum (400 MHz, $\text{CD}_3\text{CN}-d_3$) of B5.

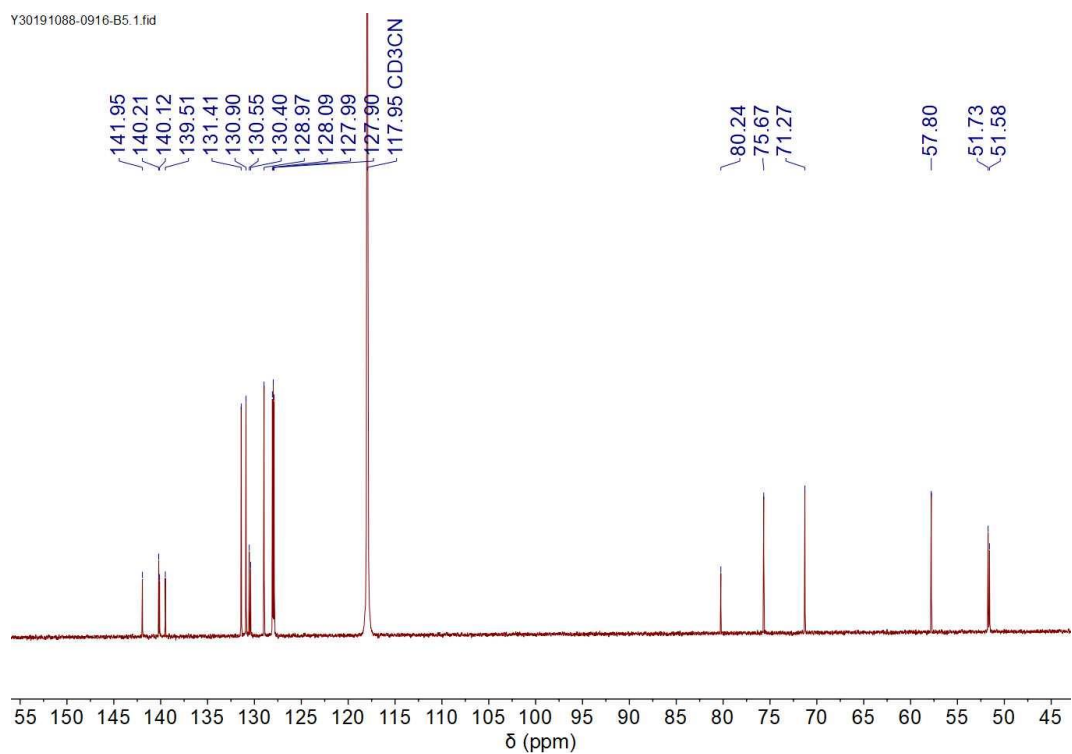


Fig. S37. ^{13}C NMR spectrum (101 MHz, $\text{CD}_3\text{CN}-d_3$) of B5.

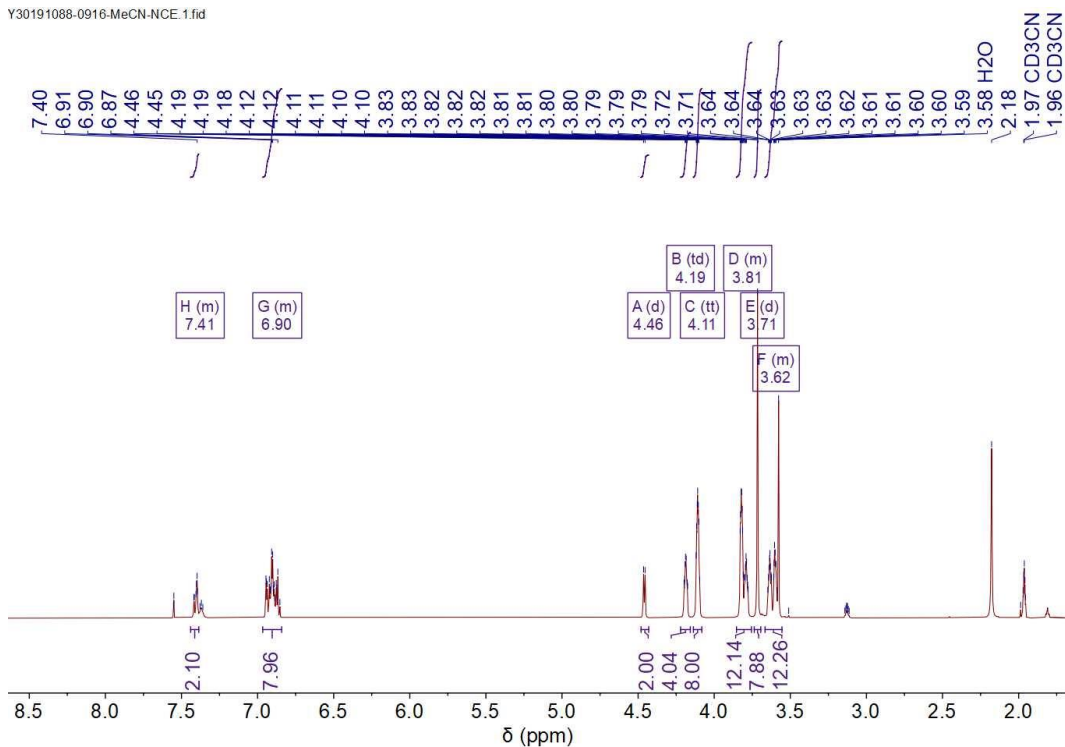


Fig. S38. ¹H NMR spectrum (600 MHz, CD₃CN-*d*₃) of NCE.

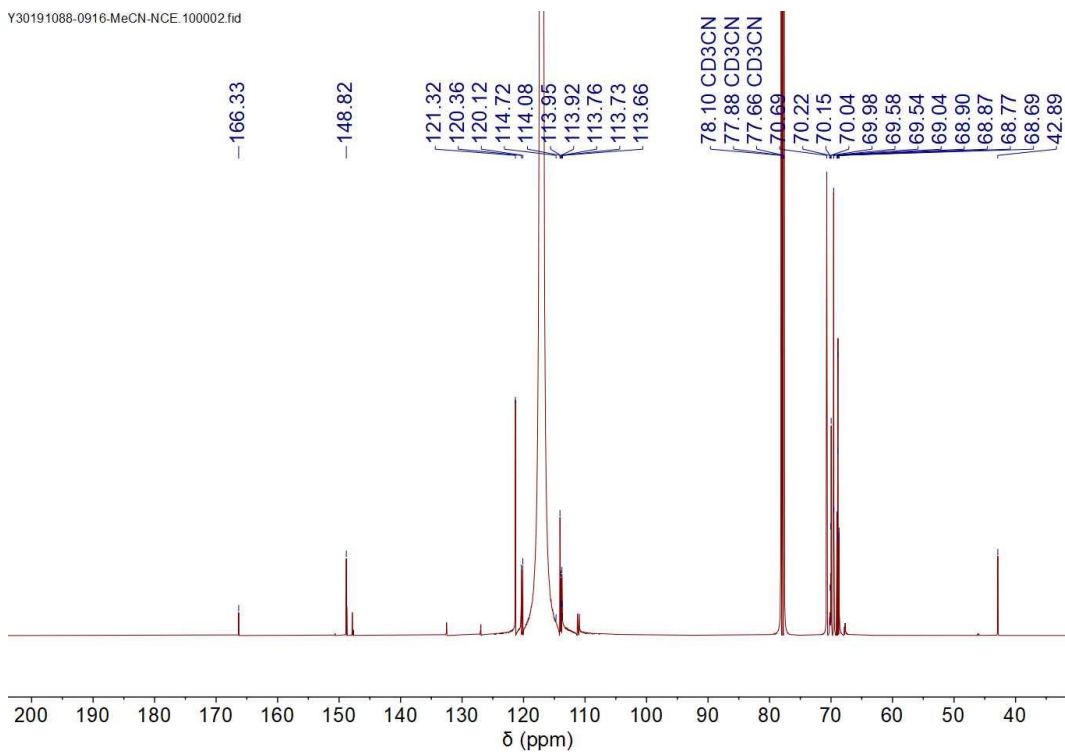


Fig. S39. ¹³C NMR spectrum (151 MHz, CD₃CN-*d*₃) of NCE.

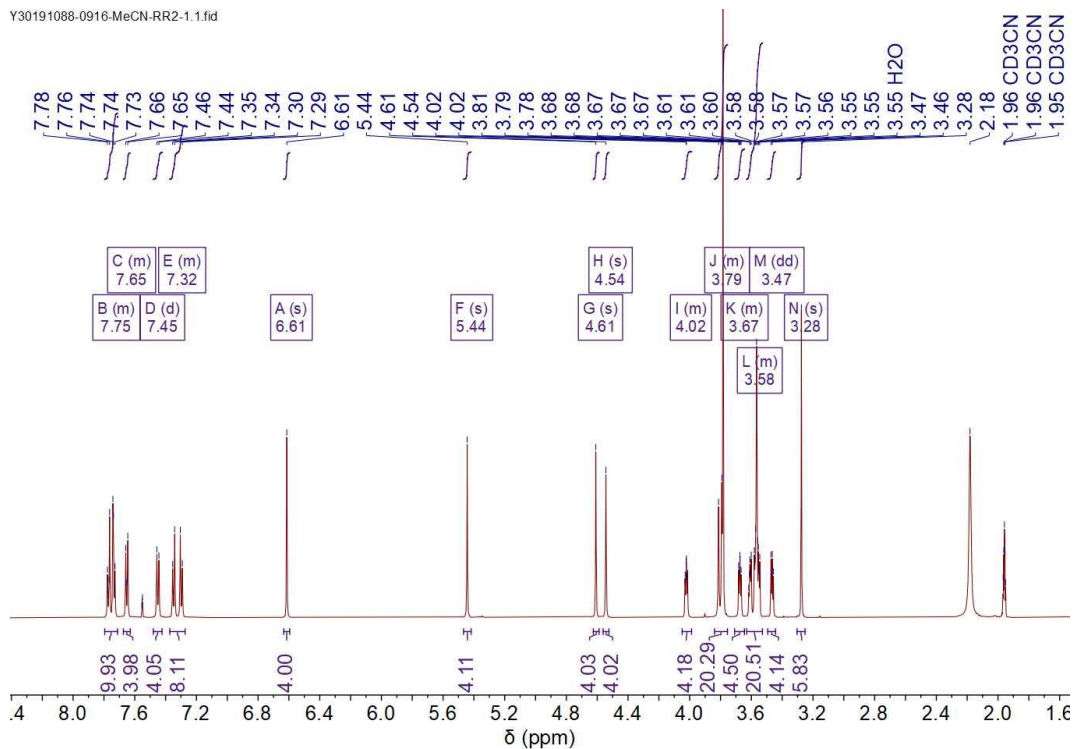


Fig. S40. ¹H NMR spectrum (600 MHz, CD₃CN-*d*₃) of RT.

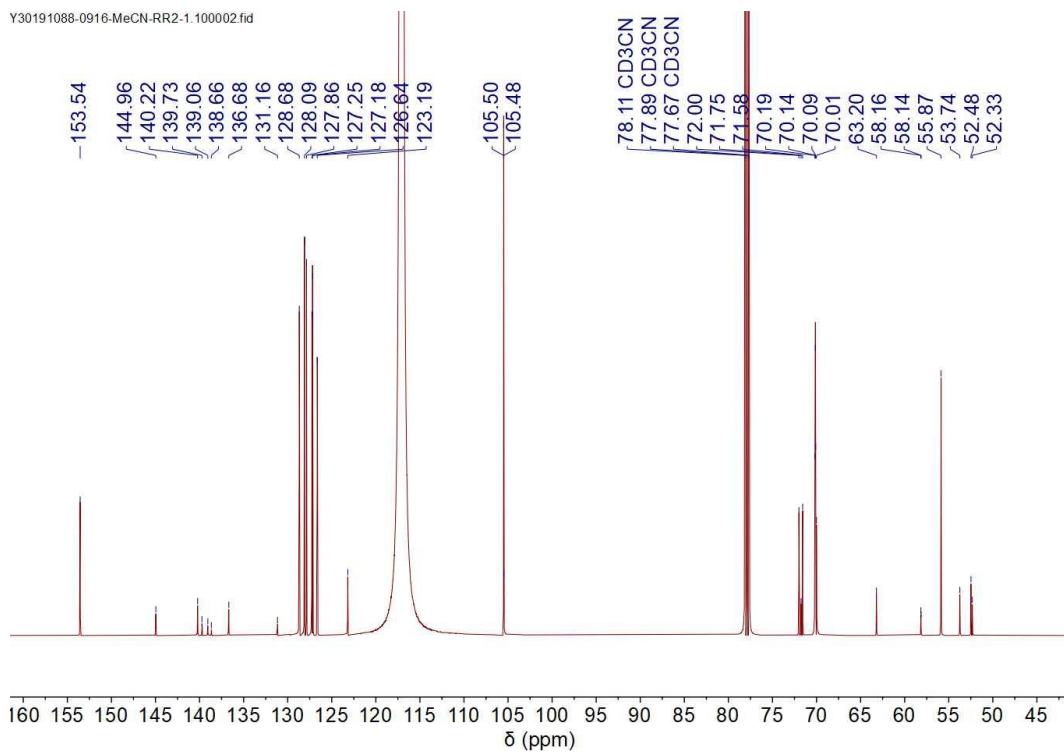


Fig. S41. ¹³C NMR spectrum (151 MHz, CD₃CN-*d*₃) of RT.

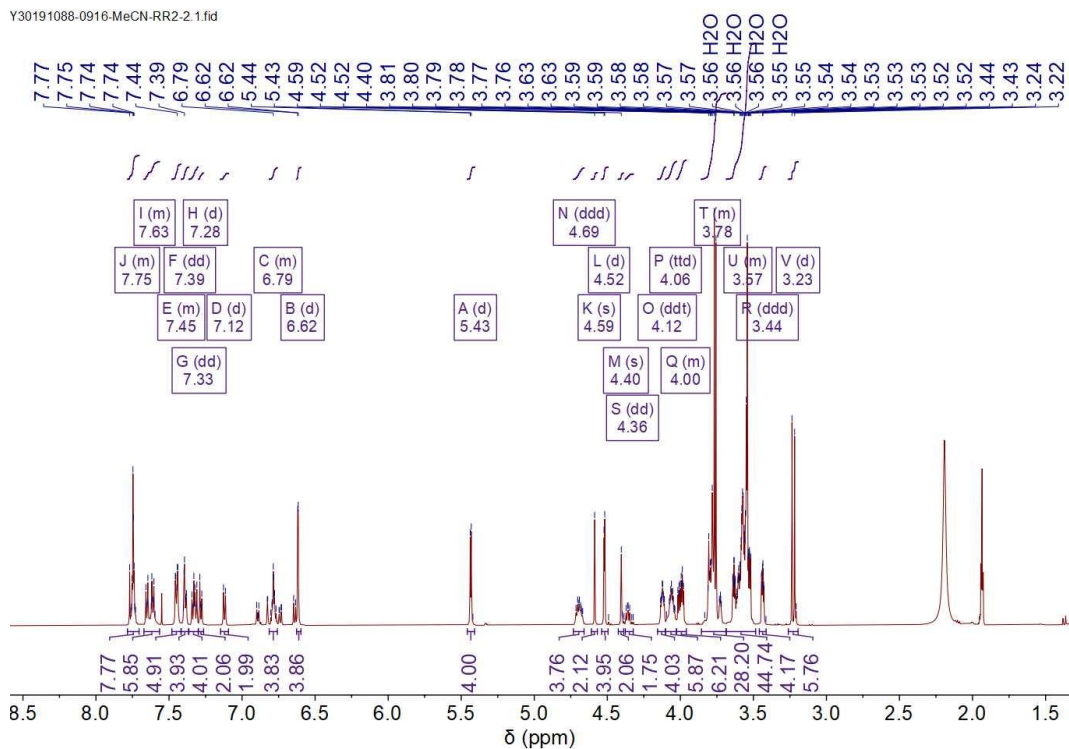


Fig. S42. ¹H NMR spectrum (600 MHz, CD₃CN-*d*₃) of RR[2].

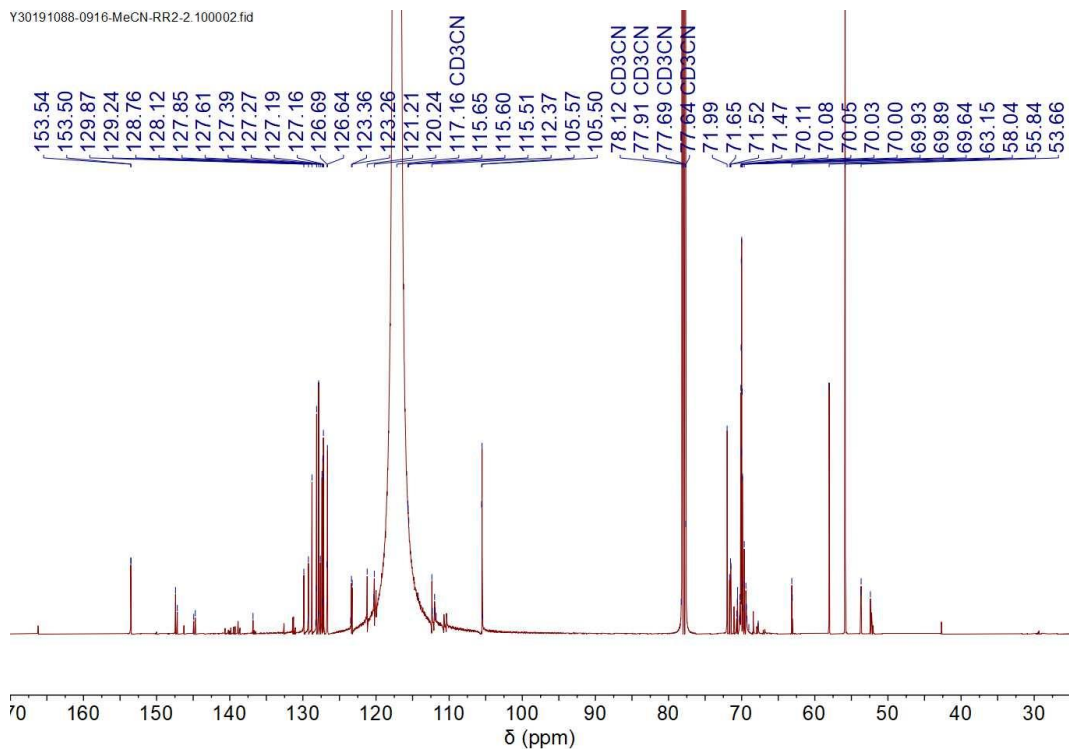


Fig. S43. ¹³C NMR spectrum (151 MHz, CD₃CN-*d*₃) of RR[2].

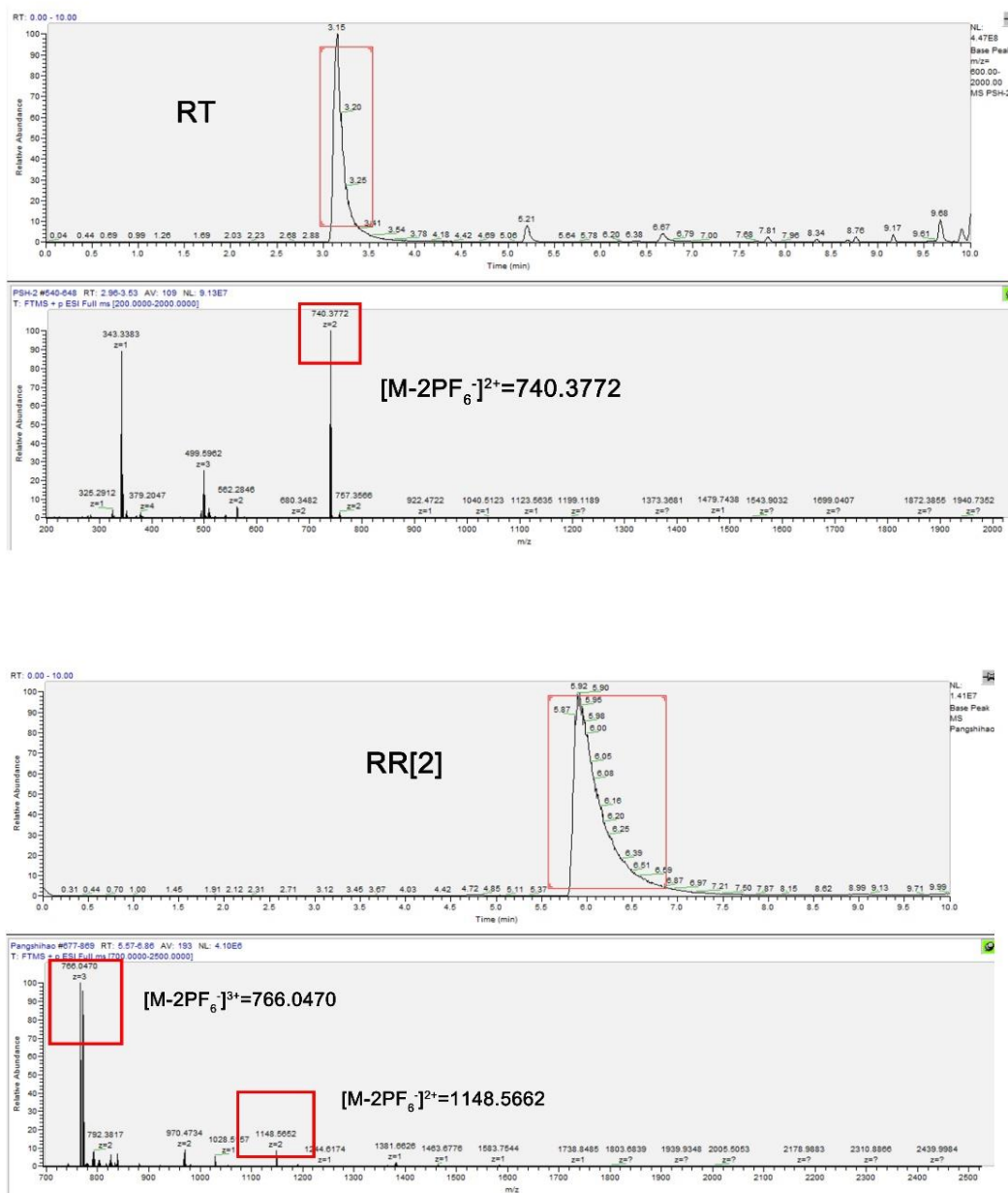


Fig. S44. LC-MS spectra for RT and RR[2].

9. References

1. Wang, C.; Wang, S.; Yang, H.; Xiang, Y.; Wang, X.; Bao, C.; Zhu, L.; Tian, H.; Qu, D. H., A Light-Operated Molecular Cable Car for Gated Ion Transport. *Angew. Chem. Int. Ed.*, **2021**, *60* (27), 14836-14840.
2. Chen, S.; Wang, Y.; Nie, T.; Bao, C.; Wang, C.; Xu, T.; Lin, Q.; Qu, D. H.; Gong, X.; Yang, Y.; Zhu, L.; Tian, H., An Artificial Molecular Shuttle Operates in Lipid

Bilayers for Ion Transport. *J. Am. Chem. Soc.*, **2018**, *140* (51), 17992-17998.

3. Young, P. G.; Hirose, K.; Tobe, Y., Axle length does not affect switching dynamics in degenerate molecular shuttles with rigid spacers. *J. Am. Chem. Soc.*, **2014**, *136* (22), 7899-7906.